

1 **Arctic sea ice algae differ markedly from phytoplankton in their ecophysiological**
2 **characteristics**

3 Ane Cecilie Kvernvik¹, Clara Jule Marie Hoppe², Michael Greenacre^{3,8}, Sander Verbiest⁴,
4 Jozef Maria Wiktor⁵, Tove M. Gabrielsen^{1,6}, Marit Reigstad⁷, Eva Leu⁸

5 ¹The Department of Arctic Biology, University Centre in Svalbard, Svalbard Science Centre, N-9171
6 Longyearbyen, Norway; ²Marine Biogeoscience, Alfred Wegener Institut – Helmholtzzentrum für
7 Polar- und Meeresforschung, 27570 Bremerhaven, Germany; ³Department of Economics and
8 Business, Universitat Pompeu Fabra and Barcelona Graduate School of Economics, Ramon Trias
9 Fargas 25-27, 08005 Barcelona, Spain; ⁴Department of Earth Sciences, Faculty of Geosciences,
10 Utrecht University, Utrecht 3584 CB, The Netherlands; ⁵Institute of Oceanology, Polish Academy of
11 Sciences, 81-712 Sopot, Poland; ⁶Department of Natural Sciences, University of Agder, 4604
12 Kristiansand, Norway; ⁷Department of Arctic Marine Biology, The Arctic University of Norway, 9019
13 Tromsø, Norway; ⁸Arctic R&D, Akvaplan-niva AS, Fram Centre, 9296 Tromsø

14
15 Author for correspondence:

16 *Ane Cecilie Kvernvik*

17 *Tel: +47 98018439*

18 *Email: anek@unis.no*

19

20 Running head: Ecophysiological characteristics of Arctic microalgae

21

22 This article has been accepted for publication and undergone full peer review but has not been
23 through the copyediting, typesetting, pagination and proofreading process, which may lead to
24 differences between this version and the version of record. Please cite this article as doi:
25 <https://doi.org/10.3354/meps13675>.

26 This article is protected by copyright. All rights reserved.

1 **Abstract**

2 Photophysiological and biochemical characteristics were investigated in natural communities
3 of Arctic sea ice algae and phytoplankton, to understand their respective responses towards
4 variable irradiance and nutrient regimes. This study revealed large differences in
5 photosynthetic efficiency and capacity between the two types of algal assemblages. Sea ice
6 algal assemblages clearly displayed increased photoprotective energy dissipation under the
7 highest daily average irradiance levels ($> 8 \mu\text{mol photons m}^{-2} \text{ s}^{-1}$). On the contrary,
8 phytoplankton assemblages were generally light limited within the same irradiance ranges.
9 Furthermore, phytoplankton assemblages exhibited more efficient carbon assimilation rates in
10 the low irradiance range compared to sea ice algae, possibly explaining the ability of
11 phytoplankton to generate substantial under-ice blooms. They also were able to readily adjust
12 and increase their carbon production to higher irradiances. The Arctic is warming more
13 rapidly than any other oceanic region on the planet, and as a consequence, irradiance levels
14 experienced by microalgae are expected to increase due to declining ice thickness and snow
15 cover, as well as enhanced stratification. The results of this study suggest that sea ice algae
16 may have less capacity to adapt to the expected environmental changes compared to
17 phytoplankton. We therefore anticipate a change in sea ice-based vs. pelagic primary
18 production with respect to timing and quantity in a future Arctic. The clearly distinct
19 responses of sea ice algae vs. phytoplankton need to be incorporated into model scenarios of
20 current and future Arctic algal blooms and considered when predicting implications for the
21 entire ecosystem and associated biogeochemical fluxes.

22

23 **Key words:** Sea ice algae, Phytoplankton, Photoacclimation, Carbon fixation, Light, Nitrate,
24 Primary production, Climate change

1 **1. Introduction**

2 In the ice-covered seas of the Arctic, two major functionally distinct types of primary
3 producers are found: Sea ice algae (i.e. living within or closely attached to sea ice), and
4 phytoplankton (i.e. living in the water-column, Leu et al. 2015). Sea ice algae are a key
5 component of the Arctic food web, contributing up to 57 % of total primary production in the
6 central Arctic Ocean and between 3 and 25 % in Arctic shelf regions (Legendre et al. 1992,
7 Gosselin et al. 1997, Arrigo et al. 2010, Loose et al. 2011). Sea ice algal production typically
8 peaks in early spring when phytoplankton production is thought to still be very low, extending
9 the total period of primary production in spring (Cota et al. 1991, Legendre et al. 1992).
10 Furthermore, many Arctic marine organisms have adapted their life cycles to take advantage
11 of this high-quality food source prior to the phytoplankton bloom (Runge et al. 1991, Søreide
12 et al. 2006, Søreide et al. 2010, Daase et al. 2013). Growth and succession in both sea ice and
13 phytoplankton communities are controlled by several environmental variables: most
14 importantly, irradiances and nutrient availability (Tremblay & Gagnon 2009, Arrigo et al.
15 2014, Lewis et al. 2018), but also other drivers such as temperature and salinity (Coello-
16 Camba et al. 2015, Torstensson et al. 2015). These physical factors vary greatly over time and
17 space, and strongly influence physiology, abundance, biomass and taxonomic composition of
18 differently adapted algal communities (Sakshaug 2004, Litchman & Klausmeier 2008).

19
20 Due to the contrasting physico-chemical environments in sea ice and open water, sea ice algae
21 and phytoplankton exhibit specific adaptations to their respective habitats (Poulin et al. 2011,
22 Kvernvik et al. 2020). Irradiance reaching the bottom of sea ice is principally regulated by ice
23 thickness and overlaying snow cover, where the latter is usually most important due to its
24 high light attenuation properties (Gosselin et al. 1990, Mundy et al. 2005, Marks & King
25 2014, Hancke et al. 2018). As a result, reported transmittance through ice and snow layers in

1 the Arctic is often very low (between 0.023 – 9 % of incident irradiance; Leu et al. 2010, Leu
2 et al. 2015, Campbell et al. 2016, Assmy et al. 2017, Hancke et al. 2018). Since sea ice algae
3 live in a spatially restricted environment that is normally not undergoing rapid change, they
4 usually experience rather gradually changing irradiances of low amplitudes (i.e. gradual
5 changes in the sun's elevation, snow cover overlaid by diurnal fluctuation and variations in
6 cloud cover). Concomitantly, sea ice algal communities are facing quite challenging growth
7 conditions, such as sub-zero temperatures, high salinities, and rapidly depleted nutrient and
8 dissolved inorganic carbon (DIC) levels due to limited resupply and locally high densities of
9 algal cells (Weeks & Ackley 1986, McMinn et al. 2014, Hill et al. 2018). In comparison,
10 vertical mixing of phytoplankton cells within varying mixed surface layers implies strong and
11 rapid fluctuations in light and sometimes nutrient regimes (MacIntyre et al. 2000), while
12 salinity and DIC availability remain relatively stable. Phytoplankton species occurring in this
13 environment can therefore be expected to cope better with dynamic light conditions.

14
15 Microalgae have evolved several mechanisms that allow them to acclimate to changes in
16 irradiance, described as photoprotection and photoacclimation. The most important short term
17 (seconds-hours) photoprotective mechanisms involve increased non-photochemical quenching
18 (NPQ) of excitation energy, which in diatoms is mainly driven by the de-epoxidation of
19 xanthophyll cycling (e.g. diadinoxanthin and diatoxanthin; Lacour et al. 2020). On longer
20 time scales (hours-days), microalgae can alter cellular pigment composition, e.g., by
21 increasing antioxidant carotenes and xanthophylls as well as decreasing the light harvesting
22 pigments in response to high irradiance (Brunet et al. 2011). Despite the ability of microalgae
23 to acclimate to increasing irradiances, high light levels at potentially species-specific
24 thresholds can still have negative physiological effects resulting in high light stress and
25 photoinhibition (Barlow et al. 1988, Galindo et al. 2017). This can be a result of cells mostly

1 acclimating to their average experienced growth environment, which is substantially lower
2 than the experienced peak values (Behrenfeld et al. 1998, Van De Poll et al. 2005).
3 Furthermore, photoacclimation by adjusting pigmentation takes more time (hours to days),
4 hence, responding to rapidly increasing irradiances may remain a challenge for some algae at
5 shorter time scales (Leu et al. 2006, Kvernvik et al. 2020).

6
7 Seasonally ice-covered seas at high latitudes are characterized by very pronounced algal
8 spring blooms, usually starting with a sea ice bloom followed by a phytoplankton one. During
9 the early stages when nutrients are plentiful, microalgal growth is often primarily limited by
10 light (Leu et al. 2015). Later, because of intense algal growth during bloom events, inorganic
11 nutrients become gradually depleted, and turn into a limiting factor for further biomass
12 accumulation (Hansell et al. 1993, Varela et al. 2013, Danielson et al. 2017). In coastal Arctic
13 regions, nitrogen is the main limiting nutrient (Strom et al. 2006, Van De Poll et al. 2016),
14 which is often reflected in high carbon to nitrogen (C:N) ratios in microalgae (Niemi &
15 Michel 2015). Nitrogen starvation may have considerable effects on microalgal
16 photophysiology, because synthesizing proteins for photo-repair (such as D1 in the
17 photosynthetic reaction center and Rubisco) and pigments for photoacclimation require high
18 nutrient levels (Geider et al. 1993, Eberhard et al. 2008). Moreover, under nutrient limitation a
19 larger proportion of energy derived from light reactions may be used for nutrient uptake rather
20 than carbon fixation (Kulk et al. 2018). Hence, NO_3^- limitation can impede photoacclimation
21 responses and increase the susceptibility to photoinhibition at high irradiance (Lewis et al.
22 2018). This is critical, since during the period of nutrient depletion, algal communities might
23 also be exposed to high levels of irradiance as snow and ice melt (Nicolaus et al. 2012).

24

1 The Arctic is warming more rapidly than any other oceanic region on the planet, leading to a
2 reduction in sea ice extent and thickness (Kwok et al. 2009, Screen et al. 2011), earlier sea ice
3 melt onset (Nicolaus et al. 2012), and declining snow cover (Screen & Simmonds 2012), in
4 addition to amplified river discharge due to increasing precipitation and terrestrial ice melt
5 (Peterson et al. 2002). Since the underwater light climate in the high Arctic is primarily
6 regulated by snow and ice cover (Mundy et al. 2005, Aumack & Juhl 2015), the Arctic Ocean
7 is expected to shift from a predominantly light-controlled (ice-covered) to a more nutrient-
8 controlled (open water) system (Carmack & Wassmann 2006). This may not only affect the
9 physiological performance, but also competitiveness and biochemical characteristics of
10 microalgae. Therefore, we expect major changes in microalgal community structure,
11 succession and bloom phenology in the Arctic (Rat'kova & Wassmann 2002, Hegseth &
12 Sundfjord 2008, Nöthig et al. 2015, Ardyna & Arrigo 2020), with potentially cascading
13 effects at higher trophic levels. Sea ice and phytoplankton blooms do not only differ with
14 respect to seasonal timing, but are also utilized by different groups of grazers – which will
15 likely result in clearly distinct effects on higher trophic levels, when their relative contribution
16 to Arctic primary production is altered (Søreide et al. 2010, Huntington et al. 2020). For
17 developing realistic future scenarios, a proper mechanistic understanding of the physiological
18 and biochemical responses of sea ice algae and phytoplankton towards their changing
19 environment is essential. Of particular importance in this context is to understand how the
20 balance between sea ice vs. phytoplankton primary production will change with respect to
21 timing and quantity.

22

23 The aim of this study was to compare photophysiological and biochemical characteristics of
24 natural sea ice algal vs. phytoplankton communities and identify their response to changes in
25 the environment. To this end, we collected time series data of sea ice algae and phytoplankton

1 from a high Arctic fjord, taking advantage of the rare co-occurrence of their respective spring
2 blooms to conduct field experiments. We hypothesized that sea ice algae and phytoplankton
3 displayed distinct differences in their responses towards changes in their abiotic environment,
4 and expected sea ice algal communities to be less resistant towards high light stress compared
5 to phytoplankton communities – as a result of their adaptation to two very different habitat
6 types.

7

8 **2. Materials and methods**

9 *2.1. Study area*

10 This study was conducted in Van Mijenfjorden, an approximately 10 km wide and 50 km long
11 fjord located on the west coast of Spitsbergen, Norway (Fig. 1). The mouth of the fjord is
12 largely closed off by the island Akseløya, which together with a shallow sill (< 30m) limits
13 the exchange of fjord water with the warm and saline Atlantic water from the West
14 Spitsbergen Current. Furthermore, the rather closed nature of the fjord leaves it less exposed
15 to winds and waves, which offers favorable conditions for the formation of a stable sea ice
16 cover. The fjord can be divided into an outer basin, which is ~10 km wide and 100 m deep,
17 and an inner basin, which is 5 km wide and has an average depth of ~30 m (Kangas 2000).
18 Time for freeze-up usually covers a wide time span ranging from November to January, while
19 the ice normally breaks up between June and July depending on ice coverage and thickness
20 (Høyland 2009).

21

22 *2.2. Sample collection*

23 Samples of sea ice algae and phytoplankton were collected from ice cores and in the water
24 column from a total of eight stations in Van Mijenfjorden (Vmf) between March and August
25 2017 (Fig. 1). Detailed information on stations, sampled depth, snow and ice thickness,

1 irradiance, salinity, NO_3^- levels and temperature are shown in Table 1. Sea ice samples for
2 community composition, elemental analysis and photosynthetic pigments were collected from
3 the bottom 3 cm of sea ice cores using a Kovacs Mark2 core barrel (9 cm diameter; Kovacs
4 Enterprise, Roseburg, USA). On each sampling day, three sets of six cores each were taken
5 approximately one meter apart. To compare the effect of the different snow depths on sea ice
6 algae, on the 23rd and 26th of April and on the 2nd of May samples were taken from areas with
7 low (0-5 cm) and high (20+ cm) snow cover. Snow depth and ice thickness for each core were
8 recorded and averaged. Samples for filter-based bulk analyses were left for melting in
9 darkness over 24 h (5-10°C), after adding 100 mL of GF/F filtrated sea water per cm of core
10 to minimize osmotic stress (Bates & Cota 1986, Garrison & Buck 1986). After thawing, the
11 volume of the samples was measured and sets of six cores were pooled together in order to
12 obtain three pools per station and per treatment in the case of low vs. high snow depth. From
13 each pool water was analyzed for community composition and filtered for pigment analysis
14 (HPLC), particulate organic carbon and nitrogen (POC, PON) and chlorophyll (Chl) *a* (see
15 detailed description below). From each sampling event (date, station and low vs. high snow
16 depth) five additional ice cores were taken: Three for photo-physiological measurements, one
17 was left to thaw without the addition of filtered seawater, to be used for nutrient analysis and
18 one was used to measure ice temperature and left to thaw without addition of filtered sea
19 water for salinity measurements (see detailed descriptions below). Phytoplankton sampling
20 was performed using a 10 L Niskin bottle (Ocean Test Equipment Inc., Fort Lauderdale, Fla.,
21 USA) at different depths; 0m, 5m, 15m, 25m and 50m. Water from each depth was analyzed
22 for community composition and filtered for pigment analysis (HPLC), particulate organic
23 carbon and nitrogen (POC, PON) and chlorophyll (Chl) *a* (see detailed description below).
24 From each sampling event (date and station), additional niskin bottles were taken at 0m (ice-

1 based sampling only), 5m, 25m and 50m for photo-physiological measurements (see detailed
2 description below).

3

4 *2.3. Environmental parameters*

5 Planar incoming and downwelling photosynthetically active radiation (PAR; 400-700nm) was
6 measured simultaneously at every sampling site and date between 11:00 and 13:00 h in Van
7 Mijenfjorden, using two cosine-corrected 2π sensors (LI-192) coupled to a LI-1400 data
8 logger (Li-cor, Lincoln, USA). In this study, we wanted to identify responses of sea ice algae
9 and phytoplankton towards changes in daily average irradiances, and hence calculated the
10 daily incoming PAR (PAR_{24}) retrieved from Li-Cor light sensors (Li-1800, Lincoln, USA)
11 monitoring PAR every 10 minutes in Adventdalen (~50 km north from Van Mijenfjorden).
12 However, the cloud coverage was not always similar between the two fjords on the specific
13 sampling days. Meteorological data comparing cloud coverage in addition to the incoming
14 irradiance around noon in Van Mijenfjorden and Adventdalen were therefore used to choose
15 the most similar days with respect to irradiance regimes between the two fjords (± 1 day from
16 the sampling date).

17

18 For the discrete PAR measurements at the ice-water interface in Van Mijenfjorden, one sensor
19 was placed on the sea ice surface and the other sensor directly at the underside of the sea ice
20 ~1.5 m south from the core hole using a folding L-shaped hinging arm. The incoming and
21 transmitted planar down-welling PAR was used to calculate % transmitted irradiance through
22 ice and snow depths (Table S1). In order to calculate daily average irradiance at the ice-water
23 interface (for sea ice algae), we multiplied the daily integrated PAR_{24} (see above) by the
24 calculated % transmitted PAR for the specific station and date.

25

1 Similar measurements using the two 2π PAR sensors and data logger were performed every
2 meter (ranging from 0 to 40 m) for assessment of the light climate in open water, which were
3 done from a small tender away from the larger main vessel, to reduce the shading effect of the
4 vessel. The incoming and transmitted downwelling irradiances at 1 m depth were used to
5 calculate % transmitted irradiance to surface waters, which was then multiplied by daily
6 integrated PAR₂₄ to estimate the daily irradiance in surface waters (E_0). The water column
7 diffuse attenuation coefficient (K_d) was determined based on the Beer-Lambert law
8 (Swinehart 1962). The daily irradiance at each sampling depth (E_z) was calculated using the
9 equation:

$$10 \quad E_z = E_0 * \text{Exp}^{(-K_d * Z)} \quad [1]$$

11 where E_0 is the daily surface irradiance ($\mu\text{mol photons m}^{-2} \text{ s}^{-1}$), K_d is the diffuse light
12 attenuation coefficient (m^{-1}) and Z is the sampling depth (m). For ice covered stations we used
13 the calculated daily average irradiance at the ice–water interface as E_0 .

14
15 In addition to the discrete light measurements during the sampling campaigns, we also
16 collected continuous data of integrated PAR with loggers that were a) mounted underneath the
17 sea ice as part of a sea ice observatory close to the MS, and b) part of an ocean observatory
18 close to the position of station Vmf1, to compare temporal changes in the irradiance regimes
19 at the ice-water interface and in open water. At the sea ice observatory, a Licor LI-192
20 Underwater Quantum Sensor (Licor, Lincoln, Nebraska, USA) was mounted 20 cm beneath
21 the ice-water interface (Ice thickness: 40 cm, snow depth: 3.5 cm at the time of deployment),
22 measuring integrated PAR once per hour between March 27th and May 2nd 2017. At the time
23 of retrieval, the sea ice thickness above the sensor was appx. 30 cm and covered by 27 cm of
24 snow. Snow height was measured by a Snow Depth Buoy 2017S43 (Leu et al. 2018). The
25 ocean observatory was deployed in late August 2016 at Vmf1 and retrieved one year later. At

1 12 m depth, an upward looking cosine-corrected Satlantic PAR sensor (model 1073, Satlantic,
2 Halifax, Nova Scotia, Canada) was placed, and measured incoming irradiance every second
3 hour.

4
5 Ice temperatures were measured on every sampling date and station using a Testotherm 720
6 (Testo, Titisee-Neustadt, Germany) thermometer inside small drill holes at 5 cm intervals. Sea
7 ice bulk salinity was measured on thawed sections of the core using a Symphony SP90M5
8 conductivity meter (VWR, Radnor, USA). Brine salinities were calculated from bulk salinity
9 and ice temperature (Cox & Weeks 1986, Leppäranta & Manninen 1988). Water salinity
10 (practical salinity unit, PSU) and temperature data ($^{\circ}\text{C}$) were obtained from vertical CTD
11 profiles (MiniSTD model SD-204, SAIV AS, Bergen, Norway). Nutrient samples were
12 filtered using acid washed syringes (10% HCl, 48 hours) and GF/F filters (Whatman,
13 Maidstone, UK). Samples were stored at -20°C in 15ml acid washed Falcon tubes. After
14 thawing, the samples were analyzed colourimetrically on a QuaAAtro autoanalyzer (Seal
15 Analytical, Mequon, USA) using internal calibrations and CRMs (KANSO, Osaka, Japan) for
16 quality control. The samples were analyzed for PO_4^{3-} (limit of detection; $0.004 \mu\text{mol L}^{-1}$),
17 $\text{Si}(\text{OH})_4$ (limit of detection; $0.01 \mu\text{mol L}^{-1}$) and NO_3^- (limit of detection; $0.02 \mu\text{mol L}^{-1}$)
18 concentrations.

19 20 *2.4. Species composition of algal communities*

21 The species composition of sea ice algal and phytoplankton communities was analyzed to
22 allow investigating of potential links between structural and ecophysiological characteristics.
23 From each core section (sea ice algae) and water depth (phytoplankton), 250 mL samples
24 were collected in brown bottles preserved with a glutaraldehyde-Lugol (35%, v/v) solution
25 (Rousseau et al. 1990). As sea ice algal samples had very high biomass, 0.5 mL of sample was

1 suspended in 9.95 mL artificial seawater and left to settle in 10 mL Utermöhl chambers for
2 24h (Utermöhl 1958). Phytoplankton samples were left to settle in 10 mL Utermöhl chambers
3 for 24h. Samples were analyzed for present and dominant species under an inverted
4 microscope (Nikon TE-300) equipped with differential and phase contrasts. Samples were
5 counted under 100x and 600x magnification and identified to the lowest taxonomic level
6 possible.

7

8 *2.5. Biochemical composition of algae*

9 Samples for Chl *a* determination were filtered (20 - 500 mL depending on biomass) onto
10 GF/F filters (Whatman, Maidstone, UK) using a gentle vacuum, flash-frozen in liquid
11 nitrogen, and stored at -80 °C until further analysis. Upon analysis, Chl *a* filters were
12 extracted in 10 mL methanol ($\geq 99.9\%$) for 24 hours at +4°C in the dark (Holm-Hansen &
13 Riemann 1978) and measured on a 10-AU-005-CE Fluorometer (Turner Designs, San Jose,
14 USA). POC/N samples were filtered (50 - 600 mL depending on biomass) onto pre-
15 combusted (8 hours, 450 °C) GF/F filters and stored at -20 °C in precombusted (12 hours,
16 500°C) glass petri dishes. Prior to analysis, samples were acidified (0.2 ml of 0.2M HCl) and
17 dried for 24 hours. The samples were subsequently packed into tin capsules. Most samples
18 were analyzed on a Euro EA 3000 elemental analyzer (Hekatech, Wegberg, Germany).
19 Approximately one quarter of the samples were analyzed on a Flash EA 1112 elemental
20 analyzer (Thermo Scientific, Milan, Italy) coupled to a Delta V Advantage IRMS (Thermo
21 Scientific, Bremen, Germany), since stable isotope ratios also needed to be determined for
22 these samples (data not shown, published in Leu et al. 2020). For intercalibration of the
23 different elemental analyzers, an acetanilide standard was used. C:N ratios were corrected
24 based on the difference in atomic weight in carbon and nitrogen. Samples for pigment
25 composition (100 – 300 mL) were collected when biomass was high (between 23rd of April –

1 2nd of May for sea ice algae and between 26th of April – 23rd of August for phytoplankton, see
2 Table 1 for sampling dates). Samples were filtered onto GF/F filters (Whatman, England),
3 flash-frozen in liquid nitrogen and stored at -80 °C until analysis. Frozen filters from algal
4 cultures were extracted in a Teflon-lined screw-capped tube with 1.6 ml 95 % methanol for
5 24 h, and then re-filtered through Millipore 0.45 µm filters (Millipore, Billerica, MA, USA),
6 before the final extract was injected in the HPLC system. HPLC pigment analyses were
7 performed as described in Rodriguez et al. (2006) using a Hewlett Packard 1100 HPLC
8 system (Hewlett-Packard, Ramsey, MN, USA) with a quaternary pump and auto sampler. The
9 identification of pigments was based on retention time and the optical density (OD) spectra of
10 the pigment obtained with diode array OD detector using pigments standards (Rodriguez et al.
11 2006).

13 2.6. *Photo-physiology by fast repetition rate fluorometry*

14 Chl *a* variable fluorescence was measured using a Fast Ocean FRR fluorometer (Chelsea
15 Technologies Group, Ltd., West Molesey, UK) in combination with an Act2 system
16 (Chelsea). For sea ice algae, the bottommost 1 cm were quickly scraped off and kept in the
17 dark until sufficient brine drainage was achieved (after ~5 min). Phytoplankton were sampled
18 with Niskin bottles at different depths and put directly inside the Act2 chamber after
19 sampling. Once placed inside the FRRf, cells were dark acclimated for > 5 min, and
20 subsequently exposed to a weak measuring light to record initial fluorescence (F_0). Thereafter,
21 120 single turnover (ST) saturation flashlets (blue LED color; 450 nm) with a duration of 2 µs
22 were applied, to saturate PSII and determine maximal fluorescence (F_m) and the absorption
23 cross section of PSII (σ_{PSII} [$\text{nm}^2 \text{PSII}^{-1}$]). ST saturation flashlets were followed by 60
24 relaxation flashlets, each with 40-60 µs duration, separated by 2.4 ms intervals, to record the
25 rate of reopening of PSII reaction centers (τ_{ES} [ms]; Oxborough 2012). The maximum dark-

1 acclimated quantum yield of PSII (F_v/F_m) was then calculated as $(F_m - F_0)/F_m$ (Krause & Weis
 2 1991). To record fluorescence versus irradiance (FLC) curves, the FastAct provided 10 x 3
 3 min levels of white PAR (E_{PAR} [$\mu\text{mol photons m}^{-2} \text{s}^{-1}$]) ranging from 0 to 1500 $\mu\text{mol photons}$
 4 $\text{m}^{-2} \text{s}^{-1}$. Following actinic light periods, minimum (F_0') and maximum (F_m') fluorescence in
 5 light exposed cells were determined. Relative electron transfer rates (rETR [mol e^- (mol
 6 RCII) $^{-1} \text{s}^{-1}$]) through PSII (Cosgrove & Borowitzka 2010) were calculated as:

$$7 \quad \text{rETR} = \frac{F'_m - F'_0}{F'_m} \cdot \text{EPAR} \quad [2]$$

8 The calculated rETRs were plotted against actinic irradiance to generate FLC curves in
 9 Microsoft Excel 2010 (Microsoft corporation, Redmond, WA, USA), from which the light
 10 utilization coefficient (αETR [$\text{mol e}^- \text{m}^2$ (mol RCII) $^{-1}$ (mol photons) $^{-1}$]) and the maximum
 11 photosynthetic rate (rETR_{max} [mol e^- (mol RCII) $^{-1} \text{s}^{-1}$]) were derived using the model fit of
 12 Eilers & Peeters (1988). The photoacclimation index ($E_k\text{ETR}$ [$\mu\text{mol photons m}^{-2} \text{s}^{-1}$]) was
 13 then calculated as $\text{rETR}_{\text{max}}/\alpha\text{ETR}$. Please note that no spectral correction was applied to the
 14 data. Non-photochemical quenching of Chl *a* fluorescence (NPQ) at irradiance of 300 μmol
 15 $\text{photons m}^{-2} \text{s}^{-1}$ was calculated using the normalized Stern-Volmer coefficient, which treats the
 16 sum of non-photochemical processes present in a dark-acclimated sample (including non-
 17 radiative decay and fluorescence emission at F_m) as described in Oxborough (2012):

$$18 \quad \text{NPQ}_{300} = \frac{F'_0}{F'_m - F'_0} \quad [3]$$

19 Where F'_0 and F'_m is the minimum and maximum fluorescence in cells exposed to 300 μmol
 20 $\text{photons m}^{-2} \text{s}^{-1}$, respectively.

21

22 2.7. *In situ* photosynthesis vs. irradiance incubation

23 Measurements of ^{14}C -based net primary production (NPP) *in situ* photosynthesis-irradiance
 24 curves were carried out between 1st of May – 2nd of May 2017 on samples of natural sea ice
 25 algal and phytoplankton assemblages moored for 24 h at the ice-water interface by MS station

1 in Van Mijenfjorden, Svalbard (Fig. 1). Sea ice samples were collected from bottom 1 cm of
2 three pooled sea ice cores (snow depth: 8-9 cm), whereas phytoplankton samples were
3 collected underneath the sea ice using two 20 μm phytoplankton net hauls between 0-5 m
4 depth (KC, Denmark, 24 cm diameter). The pooled samples were diluted with 700 mL GF/F
5 filtered seawater and amended with 250 mL medium (20 mL of 50x concentrated f/2 medium
6 (Sigma-Aldrich; Gaillard and Ryther 1962) mixed with 1 L of filtrated seawater) to prevent
7 nutrient limitation during the incubation period. Final Chl *a* concentrations were 71.1 ± 6.9
8 and $71.8 \pm 7.7 \mu\text{g L}^{-1}$ for phytoplankton and sea ice algae, respectively. Triplicate samples of
9 sea ice algae and phytoplankton were collected for Chl *a* variable fluorescence measurements
10 (FRRf) before the remaining samples were split into twelve 20 ml subsamples and transferred
11 to experimental bottles (50 mL capacity) with optical coating (transmission rates: 0 – 100 %,
12 Hydro-bios, Kiel, Germany). For all NPP measurements, samples were amended with
13 $\text{NaH}^{14}\text{CO}_3$ (PerkinElmer, 53.1 mCi \cdot mmol $^{-1}$ stock) giving a final ^{14}C specific activity of 1
14 $\mu\text{Ci ml}^{-1}$. To determine the total activity in the incubations, 100 μl of radioactive sample were
15 taken out in duplicates and directly transferred to a clean scintillation vial containing 250 μl
16 ethanolamine. Experimental bottles were then placed randomly on an incubation frame
17 equipped with a PAR logger (DEFI 2-L sensor) measuring every 5th min and moored for 24 h
18 underneath the sea ice (after snow was removed from the area). After incubation, samples
19 were fixed with two drops of 37 % formaldehyde before they were filtered onto GF/F-filters,
20 acidified with 500 μl 1M HCl and left to degas overnight. Filters were then transferred into
21 scintillation vials, and six hours prior to analysis, 10 mL of scintillation cocktail (Ultima Gold
22 AB, PerkinElmer, Connecticut, USA) were added to the samples and total count vials.
23 Subsequently, they were analyzed by means of a TriCarb 2900TR scintillation counter
24 (PerkinElmer, Connecticut, USA). ^{14}C fixation rates ($\mu\text{g C} (\mu\text{g Chl } a)^{-1} \text{d}^{-1}$) were calculated
25 according to Hoppe et al. (2015). Calculated ^{14}C fixation rates were plotted against irradiance

1 to generate photosynthesis versus irradiance (PE) curves, from which the initial light limited
2 slope of the PE curve (α [$\mu\text{g C } (\mu\text{g Chl } a)^{-1} \text{ d}^{-1} (\mu\text{mol photons m}^{-2} \text{ s}^{-1})^{-1}$]) and the maximum
3 photosynthetic rate (P_{max} [$\mu\text{g C } (\mu\text{g Chl } a)^{-1} \text{ d}^{-1}$]) were derived using the model fit of Eilers &
4 Peeters (1988). The photoacclimation index (E_k [$\mu\text{mol photons m}^{-2} \text{ s}^{-1}$]) was then calculated as
5 P_{max}/α . Carbon uptake in dark was not subtracted from the clear bottles, but is shown in the
6 figure.

7

8 2.8. Statistical analysis

9 Students' t-test with data following a normal distribution (Shapiro-Wilk test) were performed
10 to evaluate significant differences between sea ice algae and phytoplankton of the
11 photophysiological and biochemical parameters from field observations and the *in situ*
12 incubation experiment (i.e. parameters shown in Table 2) using the program Sigmaplot
13 (SysStat Software, San Jose, CA, USA). Modeling of parameters as a function of irradiance
14 and NO_3^- levels was performed with generalized additive mixed modeling (GAMM), using
15 the `gamm()` function in the R package `mgcv` (Wood 2017, R Core Team 2017). Replicates for
16 phytoplankton samples were modeled as being correlated if they were taken at the same
17 station on the same day. For the sea ice samples, replicates were modeled as being correlated
18 if they were taken at the same station on the same day and with the same snow cover, either
19 low or high. All relationships were modeled as log-log ones, implying that the size effect is a
20 percentage change in the response for a given percentage change in the predictor. In many
21 cases the GAMM model diagnosed a linear relationship where the effect size was constant,
22 but in a case where the relationship was nonlinear the effect size changed depending on the
23 predictor's value. Relationships were plotted along with 95 % confidence error curves and
24 when parameters were found to be significantly related to both irradiance and NO_3^- contour

1 plots were made using the function `vis.gam()`, also in the `mgcv` package. Responses were
2 deemed significant when the p-values were < 0.05 .

3

4 **3. Results**

5 *3.1. Environmental conditions*

6 This study followed the development of sea ice algae from 9th of March to 2nd of May 2017,
7 and phytoplankton from 13th of March to 28th of August 2017 (Table 1). During the field
8 campaign in Van Mijenfjorden in 2017, air temperature mainly remained below 0°C (ranging
9 from -29 to 0 °C) between early March and early May. After 31st of May, air temperature
10 consistently stayed above 0°C (Fig. 2a). Water temperatures at 12 m (retrieved from the
11 multi-parameter ocean observatory) remained stable at ~1.8°C between early March and 30th
12 of April. Thereafter, water temperature started to increase gradually reaching temperatures >0
13 °C by the 13th of June. By the end of the field campaign (28th of August), the ocean
14 temperature had increased to 5.4 °C (Fig. 2a). Sea ice started to form in the inner basin at the
15 end of January/early February and covered the fjord out to station Vmf4 by early May. The
16 inner and outer basins were ice free from mid-June onwards (retrieved from
17 <http://polarview.met.no/>). Ice thickness remained relatively stable between stations and
18 sampling dates, ranging from 29 to 57 cm, while snow cover on sea ice was variable due to
19 wind drift as well as melting processes later in the season, and ranged from 0 to 27 cm (Table
20 1). Temporal development of ice and snow thickness from early March to early May at station
21 MS is shown in Fig. 2b.

22

23 The absolute range of daily average irradiance encountered by sampled sea ice algae was 2 -
24 74 $\mu\text{mol photons m}^{-2} \text{s}^{-1}$, with peak irradiances ranging from 12 to 305 $\mu\text{mol photons m}^{-2} \text{s}^{-1}$.
25 PAR transmittance was highly variable due to changing snow-cover, with 0.5 % transmittance

1 of incoming irradiance under the highest snow cover (27 cm) and 26 % transmittance in areas
2 without snow (Table S1). The absolute range of daily average irradiances encountered by
3 phytoplankton was 0 - 63 $\mu\text{mol photons m}^{-2} \text{s}^{-1}$ (Table 1), with peak irradiances ranging from
4 0 to 288 $\mu\text{mol photons m}^{-2} \text{s}^{-1}$. In March, daily surface irradiances in open water ranged from
5 27 (Vmf3) to 33 $\mu\text{mol photons m}^{-2} \text{s}^{-1}$ (Vmf4), with peak irradiances of 192 and 267 μmol
6 $\text{photons m}^{-2} \text{s}^{-1}$, respectively. In late April and early May, when phytoplankton sampling was
7 conducted underneath sea ice, the daily irradiance levels at the ice-water interface ranged
8 from 10 to 40 $\mu\text{mol photons m}^{-2} \text{s}^{-1}$ (with peak irradiances from 24 to 26 $\mu\text{mol photons m}^{-2} \text{s}^{-1}$
9 1). During June and August, open water stations (Vmf1 and Vmf4) were influenced by
10 meltwater and sediment loading from terrestrial runoff, leading to highly variable PAR levels
11 differing also between stations (Table 1): At Vmf4 in June the daily average irradiances at 5m
12 depth were 63 $\mu\text{mol photons m}^{-2} \text{s}^{-1}$ (with peak irradiances of 288 $\mu\text{mol photons m}^{-2} \text{s}^{-1}$), while
13 in August the daily average irradiance at 5m depth dropped to 20 $\mu\text{mol photons m}^{-2} \text{s}^{-1}$ (with
14 peak irradiances of 121 $\mu\text{mol photons m}^{-2} \text{s}^{-1}$). At Vmf1 the daily average irradiance was 1
15 $\mu\text{mol photons m}^{-2} \text{s}^{-1}$ (with peak irradiances of 6 $\mu\text{mol photons m}^{-2} \text{s}^{-1}$) in August at 5m depth.
16 Both stations had very low irradiance levels at depths below 5 m in June and August (< 1
17 $\mu\text{mol photons m}^{-2} \text{s}^{-1}$).

18
19 Regarding the temporal development of algal biomass, bottom sea ice Chl *a* concentrations
20 peaked in April with the highest concentrations found at MS the 23rd of April ($\sim 270 \mu\text{g L}^{-1}$),
21 at Vmf1 the 8th of April ($\sim 300 \mu\text{g L}^{-1}$) and at Vmf2 the 26th of April ($\sim 65 \mu\text{g L}^{-1}$, Fig. 2c). In
22 sea ice, NO_3^- levels varied strongly between dates and stations, but dropped, on average, from
23 6.6 ± 5.3 in early March to $1.0 \pm 0.9 \mu\text{mol L}^{-1}$ in early May (Table 1). Silicate and phosphate
24 levels did not change significantly over time in sea ice, ranging from 1.09 ± 0.17 to $2.28 \pm$
25 $0.21 \mu\text{mol L}^{-1}$, respectively (data not shown, available in Hoppe et al. 2020). On the 23rd (at

1 station MS) and 26th of April (at station Vmf2) and on the 2nd of May (at station MS), samples
2 were taken from areas with low (0-5 cm) and high (20+ cm) snow cover. At all tested stations
3 NO₃⁻ levels were significantly lower under low compared to high snow cover (MS on the 23rd
4 of April: students' t-test, $t_4 = 5.7$, $p = 0.004$); Vmf2 on the 26th of April: students' t-test, $t_4 =$
5 14.3, $p = 0.0001$; and Vmf2 on the 2nd of May: students' t-test, $t_4 = 4.8$, $p = 0.008$). Si(OH)₄
6 and PO₄³⁻ remained statistically similar between low and high snow sites (data not shown,
7 available in Hoppe et al. 2020). Brine temperature in the bottom 3 cm of the sea ice remained
8 relative stable (ranging from -2.0 to -1.6 °C), while brine salinity varied more, i.e. ranging
9 from 28.7 to 35.6 (Table 1). Phytoplankton Chl *a* concentrations approached ~16 µg L⁻¹
10 between 23rd of April and 2nd of May (Fig. 2c). The accumulation of phytoplankton biomass
11 resulted in a rapid drawdown of open water NO₃⁻ (from 9.9 ± 0.3 to 1.1 ± 0.6 µmol L⁻¹; Table
12 1) and Si(OH)₄ levels (from 4.4 ± 0.3 to 0.3 ± 0.2 µmol L⁻¹; data not shown, available in
13 Hoppe et al. 2020) by end of April. Phosphate concentrations decreased from averagely 0.46
14 ± 0.05 µmol L⁻¹ in early March to 0.19 ± 0.09 µmol L⁻¹ in August (data not shown, available
15 in Hoppe et al. 2020). Water salinity remained fairly stable between stations and sampling
16 dates during the field campaign (ranging from 31.2 to 34.6; Table 1).

17

18 3.2. Species composition of algal communities

19 Sea ice algal assemblages were mainly dominated by pennate diatoms (between 37 – 99 % of
20 total cell abundances) across all stations and throughout the sampling period (Fig. 3a).
21 Particularly abundant taxa were *Nitzschia frigida*, *Navicula* sp. and *Fragilariopsis* sp.. No
22 coherent trends were observed when comparing sites with low and high snow depths. The
23 phytoplankton community was much more heterogenous and variable compared to sea ice
24 algae. In April and May, three major groups were found to dominate numerically:
25 Prymnesiophytes (0-68 % of total abundance), diatoms (between 30-40 %) and dinoflagellates

1 (0-40 %, Fig. 3b). Particularly abundant taxa were the colony-forming prymnesiophyte
2 *Phaeocystis pouchetii*, the centric diatoms *Chaetoceros* sp. and *Thalassiosira* sp., and the
3 pennate diatom *Fragilariopsis* sp. In June at station Vmf4, surface layers (5m) were largely
4 dominated by one known brackish and mixotrophic genus, namely *Olisthodiscus* sp.
5 (raphidophyte, 48 % of total abundance), while the deeper depths (25 and 50 m) were
6 dominated by > 80 % *Phaeocystis pouchetii*. In August, the phytoplankton protist assemblage
7 was dominated by heterotrophic and mixotrophic cryptophytes (particularly *Teleaulax* sp.)
8 and dinoflagellates (*Gymnodinium* sp.), in addition to other unidentified flagellates.

9 10 3.3. Photophysiological and biochemical responses from field observations

11 In order to assess ecophysiological responses of natural sea ice algal and phytoplankton
12 assemblages we followed variable fluorescence characteristics, stoichiometry and pigment
13 composition of the two communities, under naturally variable environmental conditions.
14 Some responses were similar between sea ice algae and phytoplankton, such as a positive
15 correlation between the amount of the photoprotective pigments diadinoxanthin and
16 diatoxanthin per Chl *a* ((DD+DT):Chl *a* ratios) with irradiance. However, the results also
17 revealed large differences in photosynthetic efficiency and capacity between the two algal
18 assemblages, especially when daily average irradiance levels were higher than 8 μmol
19 $\text{photons m}^{-2} \text{s}^{-1}$, and NO_3^- levels were depleted ($< 0.5 \mu\text{mol L}^{-1}$).

20
21 F_v/F_m , the maximum dark-acclimated PSII quantum yield, of the sea ice algal assemblages
22 ranged from 0.05 to 0.48, and was significantly correlated with both irradiance ($p = 0.0006$)
23 and NO_3^- ($p = 0.0008$; Fig. 4a). The relation between F_v/F_m and irradiance was, however, not
24 linear. After log-transforming the different variables, we can deduce that for a 10 % increase
25 in irradiance, sea ice algal F_v/F_m increased by 3.3 % up to daily average values of $\sim 6 \mu\text{mol}$

1 photons $\text{m}^{-2} \text{s}^{-1}$. When irradiance levels increased $> 8 \mu\text{mol photons m}^{-2} \text{s}^{-1}$, sea ice algal F_v/F_m
2 started to decrease by 3.4 % for every 10 % increase in irradiance (Fig. 4b). The relation
3 between F_v/F_m and NO_3^- levels was increasing linearly (by 2.9 % for every 10 % increase in
4 NO_3^-) in sea ice algae (Fig. 4c). Hence, the lowest sea ice algal F_v/F_m values (< 0.1) were
5 observed under high irradiance ($>$ average daily irradiance of $74 \mu\text{mol photons m}^{-2} \text{s}^{-1}$, with
6 peak irradiances reaching $\sim 305 \mu\text{mol photons m}^{-2} \text{s}^{-1}$) and low NO_3^- ($< 0.5 \mu\text{mol L}^{-1}$) levels.
7 F_v/F_m of phytoplankton ranged from 0.06 to 0.55, with the highest values being observed
8 between mid-March and early May (0.32 – 0.55), when communities were dominated by
9 prymnesiophytes, diatoms and dinoflagellates (Supplementary material, Fig. S1).
10 Phytoplankton F_v/F_m was lowest in June and August, when mixotrophic and heterotrophic
11 microalgal groups dominated the assemblages (e.g. raphidophytes and dinoflagellates). By
12 then, nitrate levels were low ($< 1 \mu\text{mol L}^{-1}$) and irradiances highly variable due to high
13 sediment loads from terrestrial runoff in the innermost station, i.e. either $< 1 \mu\text{mol photons m}^{-2}$
14 s^{-1} (Vmf1) or $> 50 \mu\text{mol photons m}^{-2} \text{s}^{-1}$ (Vmf4). Phytoplankton F_v/F_m was not significantly
15 correlated with irradiance (Fig. 4e), however a slight, but non-significant positive relationship
16 was observed between F_v/F_m and NO_3^- levels (Fig. 4f). Further analysis revealed that in
17 phytoplankton communities dominated primarily by photosynthetic organisms (i.e. being
18 more similar to the sea ice algal assemblages), F_v/F_m increased slightly with increasing
19 irradiance ($p = 0.003$; data not shown). The absorption cross-section of PSII (σ_{PSII}) did not
20 show any significant trends with irradiance and NO_3^- levels in either sea ice algae or
21 phytoplankton (data not shown), and the averaged values did not differ significantly between
22 the two communities (Table 2). Similarly, no apparent trends in τ_{ES} (indicating the kinetics of
23 electron transport on the acceptor side of PSII) with changing irradiance and nutrient regimes
24 were observed in either sea ice algae or phytoplankton. However, the averaged τ_{ES} was almost
25 twice as high in the sea ice algal communities (students' t-test, $t_{52} = 3.2$, $p = 0.003$; Table 2).

1
2 Results from FRRf-based Fluorescence light curves (FLC) curves and biochemical analysis
3 revealed substantial differences in the acclimation capacity of sea ice algal and phytoplankton
4 communities. Regarding the light utilization coefficient, sea ice algae showed consistently
5 decreasing α ETR, by 3.6 % for every 10 % increase in irradiance ($p = 0.003$, Fig. 5a).
6 Moreover, in correspondence with α ETR, we observed a significant increase of
7 POC:Chl *a* content in the sea ice community with increasing irradiance levels ($p < 0.0001$,
8 Fig. 5b), where POC:Chl *a* ratios increased by 3.5 % for every 10 % increase in irradiance.
9 Contrarily, α ETR and POC:Chl *a* varied strongly in the phytoplankton communities, ranging
10 from 0.14 to 0.51 mol e⁻ m² (mol RCII)⁻¹ (mol photons)⁻¹ and from 11.9 to 1027.6 μ g C μ g
11 Chl *a*⁻¹, respectively, and the resulting relationship with irradiance was found non-significant
12 for both parameters (Fig. 5a,b). The amount of the photoprotective pigments relative to Chl *a*
13 ((DD+DT):Chl *a*) showed an increasing trend with irradiance in both sea ice algal and
14 phytoplankton assemblages (Fig. 5c). In sea ice algae, (DD+DT):Chl *a* increased by 1.3 % for
15 every 10 % increase in irradiance in the low irradiance range between 2 and 10 μ mol photons
16 m⁻² s⁻¹, and thereafter by 7.6 % ($p < 0.0001$). In phytoplankton, (DD+DT):Chl *a* ratios
17 increased by 2.7 % for every 10 % increase in irradiance, but was not found to be significantly
18 correlated. With respect to non-photochemical quenching at a measuring light intensity of 300
19 μ mol photons m⁻² s⁻¹ (NPQ₃₀₀), sea ice algae showed an increasing trend in NPQ₃₀₀ with
20 irradiance (by 4 % for every 10 % increase in irradiance), however the relationship was not
21 significant (Fig. 5d). In the phytoplankton communities, in contrast, NPQ₃₀₀ decreased
22 significantly with increasing irradiances ($p = 0.02$, Fig. 5d). Due to these two distinct
23 responses between the algal assemblages, the average NPQ₃₀₀ was significantly higher in sea
24 ice algae (13 ± 7.2) compared to phytoplankton (4.9 ± 3.2 ; students' t-test, $t_{52} = 5.3$, $p <$
25 0.0001, Table 2). Maximum electron transport rates (r ETR_{max}) were significantly correlated

1 with irradiance in sea ice algae ($p = 0.04$), however this relationship was not linear: At daily
2 average irradiance levels up to approximately $8 \mu\text{mol photons m}^{-2} \text{ s}^{-1}$, sea ice algal rETR_{max}
3 increased on average by 17.2 % per 10 % increase in light. At higher irradiances, sea ice algal
4 rETR_{max} decreased by 15.3 % for every 10 % increase in irradiance (Fig. 5e). In comparison,
5 the phytoplankton communities increased their rETR_{max} with increasing irradiances at all
6 levels $> 2 \mu\text{mol photons m}^{-2} \text{ s}^{-1}$ ($p < 0.04$), with values increasing on average by 4.0 % for
7 every 10 % increase in irradiance (Fig. 5e). Hence, the differences in rETR_{max} between the
8 two communities were substantial when irradiances increased $> 8 \mu\text{mol photons m}^{-2} \text{ s}^{-1}$,
9 resulting in higher averaged rETR_{max} in phytoplankton ($80 \pm 27 \text{ mol e}^{-} (\text{mol RCII})^{-1} \text{ s}^{-1}$)
10 compared to sea ice algae ($31 \pm 23 \text{ mol e}^{-} (\text{mol RCII})^{-1} \text{ s}^{-1}$; students' t-test, $t_{52} = 5.4$, $p <$
11 0.0001 , Table 2). The relation between rETR_{max} and NO_3^{-} levels was non-significant in both
12 algal assemblages. Similarly to POC:Chl a , C:N ratios also showed stronger environmentally
13 driven patterns in sea ice algae compared to phytoplankton. In sea ice algae, C:N ratios
14 increased by 2.2 % with a 10 % increase in irradiance ($p < 0.0001$, Fig. 6b), while decreasing
15 by 0.80 % for every 10 % increase in NO_3^{-} ($p = 0.009$, Fig. 6c). Hence, the responses were
16 strongly negatively correlated between irradiance and NO_3^{-} levels (correlation = - 0.79, Fig.
17 6a). In phytoplankton assemblages, C:N ratios were highly variable under all irradiance and
18 NO_3^{-} levels without significant trends (Fig. 6d, e, f).

19

20 3.4. *In situ* incubation experiment

21 By measuring variable fluorescence characteristics and ^{14}C -based carbon fixation *in situ* under
22 a range of different irradiances, we were able to assess differences in both the functionality of
23 the photosynthetic apparatus regarding the light-dependent reactions, as well as the ability of
24 sea ice algae and phytoplankton to fix carbon. Additional measurements (e.g. community
25 composition, *in situ* nutrients and salinity) were not taken on these specific samples on 1st of

1 May, but we assume the community and environmental conditions were similar to sampling
2 conducted on 2nd of May at that station (MS). By then, the majority of the sea ice community
3 (under high snow cover; Fig. 3a) was numerically dominated by coccal unidentified cells
4 (coccal indet; 39 %) and diatoms (36 %; particularly *Fragilariopsis* spp. and *Navicula* spp.).
5 The phytoplankton community was numerically dominated by *Phaeocystis pouchetii* (68 %),
6 centric diatoms (17 %; particularly *Chaetoceros* spp. and *Thalassiosira* spp.) and pennate
7 diatoms (13 %; particularly *Fragilariopsis* spp. and *Nitzschia* spp.; Fig. 3b). Note that
8 phytoplankton samples for the incubation experiment were sampled with a 20 μm
9 phytoplankton net, hence smaller cells probably have been largely excluded from the
10 experiment. We therefore expect the communities in the experiment to be dominated by the
11 above-mentioned diatoms as well as *P. pouchetii* (colonies) in case of the phytoplankton
12 community. *In situ* nutrient levels were depleted in both sea ice (NO_3^- : $0.67 \mu\text{mol L}^{-1}$,
13 Si(OH)_4 : $0.31 \mu\text{mol L}^{-1}$) and water (NO_3^- : $0.91 \mu\text{mol L}^{-1}$, Si(OH)_4 : $0.34 \mu\text{mol L}^{-1}$), and
14 temperature were reasonably similar between ice and water (-1.7 and -1.6 $^\circ\text{C}$, respectively;
15 Table 1). Salinity was lower in sea ice (31.4) than in water (34.6). Similar to the field
16 observation, this experiment also revealed different ecophysiological characteristics between
17 sea ice algae and phytoplankton. Before incubation under the sea ice, F_v/F_m was within the
18 same range for sea ice algae and phytoplankton, with values of 0.37 ± 0.06 vs. 0.38 ± 0.05 ,
19 respectively (Table 2). Similarly, no noticeable differences were observed with respect to the
20 rate of reopening of PSII reaction centers (τ_{ES}). The absorption cross section of PSII (σ_{PSII})
21 was slightly higher in phytoplankton compared to sea ice algal communities (students' t-test,
22 $t_3 = -3.6$, $p = 0.04$), while NPQ_{300} was significantly lower in the former (students' t-test, $t_3 =$
23 4.6 , $p = 0.02$, Table 2). Results from the FRRf-based FLC curves showed that the rETR_{max}
24 were higher in phytoplankton compared to sea ice algae (students' t-test, $t_3 = -24.5$, $p <$
25 0.001), while αETR remained similar, resulting in significantly higher FRRf-derived $E_k\text{ETR}$

1 in phytoplankton compared to sea ice algae (students' t-test, $t_3 = -4.7$, $p = 0.02$, Table 2, Fig.
2 7a. After 24 h incubation underneath the sea ice, phytoplankton showed higher carbon
3 fixation rates at all irradiances compared to the sea ice algae (Fig. 7b). Also the ^{14}C -derived α
4 in phytoplankton ($0.009 \mu\text{g C } (\mu\text{g Chl } a)^{-1} \text{ d}^{-1} [\mu\text{mol photons m}^{-2} \text{ s}^{-1}]^{-1}$) was higher compared
5 to sea ice algae ($0.004 \mu\text{g C } (\mu\text{g Chl } a)^{-1} \text{ d}^{-1} [\mu\text{mol photons m}^{-2} \text{ s}^{-1}]^{-1}$). Due to lack of light
6 saturation in the phytoplankton assemblage, ^{14}C -based P_{max} and E_k could not be derived from
7 the curve fits. In sea ice algal assemblages however, light saturation was characterized by a
8 ^{14}C -based E_k of $43 \mu\text{mol photons m}^{-2} \text{ s}^{-1}$ and a resulting P_{max} of $0.18 \mu\text{g C } (\mu\text{g Chl } a)^{-1} \text{ d}^{-1}$
9 (Table 2). Overall, the phytoplankton community showed higher mean carbon fixation rates
10 ($0.25 \pm 0.17 \mu\text{g C } \mu\text{g Chl } a^{-1} \text{ d}^{-1}$) compared to the sea ice-associated one ($0.10 \pm 0.07 \mu\text{g C } (\mu\text{g}$
11 $\text{Chl } a)^{-1} \text{ d}^{-1}$, students' t-test, $t_{22} = -2.8$, $p = 0.01$).

12

13 **4. Discussion**

14 In this study, we compared photophysiological and biochemical characteristics of sea ice algal
15 and phytoplankton communities in order to evaluate strategies used by the two functionally
16 distinct types of microalgal communities to acclimate to variations in light and nutrients.
17 According to the traditional perception, sea ice algal production peaks earlier in spring,
18 whereas phytoplankton production occurs primarily in open waters subsequent to sea ice
19 retreat (Hill & Cota 2005, Perrette et al. 2011). Increasing evidence during the recent years
20 suggests, however, a more common occurrence of phytoplankton blooms underneath sea ice,
21 which can originate from advected algal blooms in ice-free areas (Johnsen et al. 2018, Ardyna
22 et al. 2020) but have also been found to develop locally (Arrigo et al. 2012, Mundy et al.
23 2014, Assmy et al. 2017). In the current study, we found that the sea ice algal and
24 phytoplankton blooms in Van Mijenfjorden in 2017 peaked almost simultaneously (Fig. 2c).
25 Despite environmental conditions (i.e. irradiance and nutrient levels) encountered by sea ice

1 algae and phytoplankton being relatively similar in this study, we found distinct differences
2 between the two algal communities with respect to their sensitivity towards environmental
3 changes.

4

5 *4.1. Considerable requirement for photoprotection in sea ice algae*

6 Beneath the sea ice in spring when irradiance levels were low ($< 8 \mu\text{mol photons m}^{-2} \text{s}^{-1}$) and
7 nutrients were abundant, sea ice algae displayed clear signs of photoacclimation to low light.
8 The observed high F_v/F_m and αETR in combination with generally low NPQ_{300} and
9 $(\text{DD}+\text{DT}):\text{Chl } a$ ratios (Figs. 4b, 5a,c,d) suggest that there was little requirement of
10 dissipating absorbed energy as heat. This is in line with various studies that have suggested
11 specific adaptations of polar microalgae that enable them to grow under very low irradiances,
12 such as high growth rates, very high cellular Chl *a* quota and a low light saturation of
13 photosynthesis (Cota 1985, Kirst & Wiencke 1995, Lacour et al. 2017, Hancke et al. 2018).
14 As daily average irradiances increased towards $\sim 8 \mu\text{mol photons m}^{-2} \text{s}^{-1}$, significantly
15 decreasing FRRf-derived αETR and increasing POC:Chl *a* ratios support that sea ice algae
16 efficiently acclimated to higher irradiances, probably by reducing the quota of photosynthetic
17 pigments (Fig. 5a, b). Furthermore, and in line with previous work, the significant positive
18 relationships between $(\text{DD}+\text{DT}):\text{Chl } a$ ratios and irradiance in sea ice algae (Fig. 5c) confirms
19 that light transmittance exerts a strong control on carotenoids synthesis even under relatively
20 low irradiance levels (Alou-Font et al. 2013, Galindo et al. 2017). Hence, a rapid decline in
21 light harvesting coupled with increased capacity for photoprotection seems to be the preferred
22 method of balancing energy flow to PSII in sea ice algae with increasing irradiances. Given
23 the strong dominance of diatoms in the sea ice algal assemblages, which are known to
24 efficiently employ such photoprotective mechanisms, the observed responses were as
25 expected (Fig. 3a, von Quillfeldt et al. 2003, Brunet et al. 2011, Alou-Font et al. 2013, Lacour

1 et al. 2020). These light-driven adjustments to the photosynthetic machinery were effective in
2 the low average irradiance range between 0 and 8 $\mu\text{mol photons m}^{-2} \text{ s}^{-1}$, and ensured a high
3 level of plasticity in their light-acclimation capabilities: This resulted in elevated maximum
4 dark-acclimated quantum yield of PSII (F_v/F_m) and concurrently allowed for increased
5 maximum electron transport rates through PSII ($r\text{ETR}_{\text{max}}$) towards daily average irradiance
6 levels of $\sim 8 \mu\text{mol photons m}^{-2} \text{ s}^{-1}$ (Figs. 4a, b and 5e). When daily irradiance levels increased
7 beyond 8 $\mu\text{mol photons m}^{-2} \text{ s}^{-1}$, sea ice algal assemblages clearly invested more energy in
8 photoprotection: (DD+DT):Chl *a* ratios increased rapidly with increasing irradiance, and
9 NPQ₃₀₀ approached values of > 20 (Fig. 5c,d), indicating substantial photoprotective efforts.
10 This increased dissipation of excess excitation energy caused F_v/F_m and $r\text{ETR}_{\text{max}}$ to decrease
11 with increasingly higher irradiances ($> 8 \mu\text{mol photons m}^{-2} \text{ s}^{-1}$; Figs. 4b, 5e). The observed
12 decrease in $r\text{ETR}_{\text{max}}$ may also indicate photoinactivation of PSII, or that the turnover of
13 proteins associated with photoprotection (such as D1) was not sufficient to sustain high rates
14 of electron transport through PSII (Fig. 5e). Under the highest light (daily average irradiance
15 levels of $\sim 74 \mu\text{mol photons m}^{-2} \text{ s}^{-1}$, with peak irradiances of $\sim 305 \mu\text{mol photons m}^{-2} \text{ s}^{-1}$), F_v/F_m
16 reached extremely low values (0.11 ± 0.09), indicating a strong decline in photosynthetic
17 performance. It is important to note however, that the highest light often co-occurred with low
18 nutrient levels, resulting in co-occurrence and potential interaction of stressors (as discussed
19 later). We conclude that sea ice algae did not benefit from the increased light availability at
20 average daily irradiances $> 8 \mu\text{mol photons m}^{-2} \text{ s}^{-1}$ which was frequently observed from 23rd of
21 April onwards under snow cover $< 15 \text{ cm}$. This is in line with previous findings of a
22 detrimental effect of high irradiances on sea ice algal communities (Leu et al. 2010, Juhl &
23 Krembs, 2010, Alou-Font et al. 2013, Kvernvik et al. 2020).

24

1 Changing environmental conditions can cause alterations in cellular C:N ratios of microalgae,
2 deviating from Redfield ratios (Sterner & Elser 2002, Frigstad et al. 2014, Niemi & Michel
3 2015). Both irradiance and NO_3^- are known to exert strong control on C:N ratios, where
4 values may increase as a result of acclimation to high irradiances (i.e. a relative increase in
5 cellular C quota because excess light energy is drained in C fixation) or nutrient limitation
6 (i.e. a relative decrease in cellular N quota; Demers et al. 1989, Gosselin et al. 1990). In the
7 sea ice algal assemblages, C:N ratios were positively correlated with irradiance and negatively
8 correlated with NO_3^- concentrations, i.e. the highest C:N ratios were observed under high light
9 and low NO_3^- concentrations (Fig. 6a, b, c). However, since the observations from field data
10 and *in situ* experiment strongly suggests that sea ice algae were increasingly light stressed at
11 average irradiances $> 8 \mu\text{mol photons m}^{-2} \text{s}^{-1}$ and thus did not benefit from higher light
12 availability, we hypothesize that the high C:N ratios were primarily resulting from increasing
13 nutrient limitation. Synthesis of proteins and pigments required for photoacclimation and
14 photo-repair consumes large amounts of nutrients (Eberhard et al. 2008). Congruently,
15 nutrient limitation (in particular NO_3^-) can have a pronounced effect on photosynthetic
16 performance by restricting quantum yield, photochemical efficiency of photosystem II and
17 growth (Geider et al. 1993, Van De Poll et al. 2005) in addition to increasing susceptibility to
18 photoinhibition (Kiefer 1973, Litchman et al. 2002). The highest F_v/F_m of sea ice algae in this
19 study was observed when light was low (i.e. $\sim 5 \mu\text{mol photons m}^{-2} \text{s}^{-1}$) and NO_3^-
20 concentrations were high ($> 10 \mu\text{mol L}^{-1}$). The abundant NO_3^- supplies probably supported
21 biosynthesis of photosynthetic pigments (Eberhard et al. 2008, Lewis et al. 2018), and thus
22 enhanced absorption of the limited light available beneath the sea ice. Furthermore,
23 indications of high light stress in sea ice algal assemblages were particularly pronounced
24 when nutrient levels were low, as F_v/F_m decreased to ~ 0.1 under high light ($> 50 \mu\text{mol}$
25 $\text{photons m}^{-2} \text{s}^{-1}$) and low nitrate levels ($< 0.5 \mu\text{mol L}^{-1}$, Fig. 4a). Hence, nutrient limitation

1 probably impeded photoacclimation to these higher irradiances during the later stages of the
2 sampling period and contributed to the strongly reduced photosynthetic efficiency in sea ice
3 algal assemblages, hinting towards an interactive effect between irradiance and nutrient levels
4 (Lewis et al. 2018).

5

6 *4.2. Phytoplankton exhibited a high plasticity towards variable irradiances*

7 Compared to the sea ice algal assemblages, trends in the response to variations in irradiance in
8 phytoplankton were less pronounced in several parameters such as $rETR_{max}$, photoprotective
9 pigment content ((DD+DT):Chl *a*), and NPQ₃₀₀, and even absent in several measured
10 parameters, e.g. in F_v/F_m , αETR , POC:Chl *a* and C:N ratios. As the species composition of the
11 phytoplankton communities were more heterogeneous compared to the Sea ice communities
12 (i.e. often mixed between phototrophic and mixotrophic species), and also varied more both in
13 space and time with respect of dominant groups, these lacking trends could in part be
14 explained by community shifts as discussed later.

15 It seems that light harvesting of both sea ice algae and phytoplankton was acclimated to the
16 same irradiance range (evidenced by similar averaged $E_k ETR$; Table 2), but that
17 phytoplankton showed overall higher production rates as both the averaged αETR and
18 $rETR_{max}$ were higher compared to sea ice algae, and as also indicated by the results of the
19 ¹⁴C-based production experiment (Table 2). This difference may be explained by the fact that
20 αETR and $rETR_{max}$ of phytoplankton remained similar over the entire range of irradiance
21 levels that occurred over the study period, which was in strong contrast to the sea ice algae,
22 which substantially lessened electron transport rates in response to increasing irradiances (Fig.
23 5a,e). Several of the abundant phytoplankton classes in this study possess the diadinoxanthin
24 cycle (i.e. diatoms, dinoflagellates and prymnesiophytes; Lacour et al. 2020). Similar to the
25 sea ice algae, (DD+DT):Chl *a* ratios increased with irradiance in phytoplankton as well,

1 however, this did not translate into increased NPQ₃₀₀. Consequently, NPQ₃₀₀ was twice as
2 high in sea ice algae compared to phytoplankton at higher irradiances (Fig. 5d), confirming
3 that within the same irradiance range, phytoplankton experienced much less photochemical
4 stress and relied less on photoprotection compared to sea ice algae. The absorption cross-
5 section of PSII light harvesting antenna, σ_{PSII} , (i.e. energy delivery to PSII), observed in our
6 field samples remained in a similar range in both sea ice algae and phytoplankton. The rate of
7 reopening of PSII reaction centers, τ_{ES} , however was significantly lower in the latter (Table
8 2), indicating that phytoplankton exhibited higher capacity to direct the energy away from
9 PSII (Sakshaug et al. 1997). Substantially more efficient electron drainage in an Arctic
10 pelagic compared to a sea ice diatom exposed to high light have also been found in
11 experiments with unialgal cultures (Kvernvik et al. 2020). This efficient energy drainage into
12 carbon fixation in phytoplankton, which is also seen in the overall higher carbon production in
13 phytoplankton compared to sea ice algae in the *in situ* incubation experiment during the main
14 bloom period (Fig. 7), may help to prevent high-light stress of the photosynthetic apparatus by
15 draining energy into the Calvin Cycle. This possibly explains the lower NPQ₃₀₀ values
16 observed in phytoplankton compared to sea ice algae. We speculate that, while the light levels
17 tested in this study generally did not cause signs of high light stress in phytoplankton, the
18 synthesized photoprotective pigments serve to allow them to deal with further increases in
19 irradiances. The results outlined above clearly indicate that phytoplankton possessed a high
20 plasticity towards increasing irradiances. Based on our data, it seems that phytoplankton
21 achieved successful biomass buildup via acclimatory processes downstream of PSII, while sea
22 ice algae had to rely on photoprotection within the same irradiances and thus did not benefit
23 from increased light availability at daily average irradiances $> 8 \mu\text{mol photons m}^{-2} \text{s}^{-1}$.

24

1 In sea ice algal assemblages, NO_3^- limitation affected photophysiology and contributed to the
2 strongly reduced photosynthetic efficiency in high light/low nutrient environments. In
3 phytoplankton assemblages, however, no notable trends in physiological or biochemical
4 parameters were observed with decreasing NO_3^- concentrations. For example, POC:Chl *a* and
5 C:N ratios were very variable (ranging from 12 to 1027 $\mu\text{g C } \mu\text{g Chl } a^{-1}$ and 2 – 19 mol mol^{-1} ,
6 respectively, Figs. 5b, 6e) with no clear trends for either with NO_3^- levels. Phytoplankton
7 assemblages encounter more nutrient resupply on small scales (e.g. from turbulence; Henley
8 et al. 2020) than those growing in the more enclosed sea ice realm, meaning that even though
9 the measured nutrient concentrations were similarly low in ice and open water, nutrient
10 limitation was probably still more pronounced over longer time for the sea ice algal
11 assemblages. Furthermore, POC concentrations have been shown to be largely decoupled
12 from Chl *a* concentrations when heterotrophic/mixotrophic production significantly
13 contributes to organic carbon stocks (Niemi & Michel 2015). Given the heterogenous
14 phytoplankton community composition, which was also changing dynamically, this could
15 explain the highly variable POC:Chl *a* and C:N, and subsequent lacking trends with irradiance
16 and NO_3^- levels in this study (Frigstad et al. 2014). It must be kept in mind that Chl *a* is a
17 measure of microalgae, while POC comprises microalgae, hetero- and mixo-trophic protists,
18 zooplankton and detritus. Given the very high POC:Chl *a* values in some phytoplankton
19 samples, some of this carbon might be associated with other species than phytoplankton
20 and/or detrital carbon, affecting the relationship of both POC:Chl *a* and C:N ratios with
21 irradiance and NO_3^- levels. This seems to be true especially in late summer, when mixo- and
22 hetero-trophic species and zooplankton biomass typically increase (Willis et al. 2006). As
23 algal-specific POC is difficult to sample and was not measured in this study, this limits the
24 confidence in statements purely based on these ratios. Due to their congruence with other

1 measured parameters, they still serve as a valid proxy during the phototrophically dominated
2 spring period (24th of April – 13th of June in this study).

3

4 4.3. Field observations are validated by the *in situ* incubation experimental data

5 The field observations indicate that phytoplankton exhibited higher plasticity towards
6 increasing irradiances compared to sea ice algae, which was further corroborated by the *in situ*
7 incubation experiment conducted underneath the sea ice during the main bloom period in both
8 habitats (Fig. 7a,b, Table 2). It should be emphasized that the phytoplankton samples were
9 filtered through a 20 µm net, and as we did not assess taxonomic composition on these
10 specific samples, some caution must be taken in comparing the results between the *in situ*
11 incubation experiment and field measurements. One can, however expect that the *in situ*
12 taxonomic composition in sea ice and water at MS was similar between 1st and 2nd of March
13 (Fig. 3a,b), and that the filtering of phytoplankton samples through a 20 µm net definitely had
14 a larger effect and increased the dominance of larger (i.e. diatoms and *Phaeocystis pouchetii*
15 colonies) relative to smaller cells. The photoacclimation index, E_k , is an indication of the
16 irradiance level that microalgae are acclimated to (Sakshaug et al. 1997). In phytoplankton,
17 the FRRf-derived E_{kETR} during the experiment was higher ($274 \mu\text{mol photons m}^{-2} \text{s}^{-1}$) than in
18 sea ice algae ($120 \mu\text{mol photons m}^{-2} \text{s}^{-1}$; Table 2), and in fact, higher than peak irradiances
19 during the incubation period ($\sim 200 \mu\text{mol photons m}^{-2} \text{s}^{-1}$; Fig. S2), which could be explained
20 by high plasticity in photosynthetic performance of phytoplankton (Assmy et al. 2017).
21 Furthermore, the ¹⁴C-derived PE curve (Fig. 7b) revealed that primary production in
22 phytoplankton was light limited at all applied irradiances, which indicate that the ¹⁴C-based E_k
23 was higher in phytoplankton compared sea ice algae ($43 \mu\text{mol photons m}^{-2} \text{s}^{-1}$). It should be
24 mentioned that for sea ice algae, the FRRf-derived parameters were measured directly after
25 sampling (in-ice conditions) while the ¹⁴C-derived parameters were measured after incubation

1 underneath the sea ice (under-ice conditions). Hence sea ice algae may have acclimated to
2 lower irradiance in the under-ice environment during the incubation, contributing to the three
3 times lower ^{14}C -based E_k compared to $E_{k\text{ETR}}$. In view of the high FRRf-derived E_k , the non-
4 saturating ^{14}C -based PE curve and the continuously increasing FRRf-derived $r\text{ETR}_{\text{max}}$ from
5 the field observations, we conclude that the phytoplankton tended to be generally light limited
6 throughout this study. Surprisingly, the *in situ* incubation experiment also revealed that
7 phytoplankton were more efficient in utilizing low irradiances for carbon fixation compared
8 to sea ice algae (Fig. 7b), possibly explaining the ability of phytoplankton to generate
9 substantial blooms beneath sea ice (Mundy et al. 2014, Assmy et al. 2017, Ardyna et al.
10 2020). In addition, while the FRRf-based αETR was similar in sea ice algae and
11 phytoplankton, ^{14}C -based α was twice as high in the latter. Taking into account that sea ice
12 algae may also have acclimated their photosynthetic machinery to lower light during the
13 incubation (and therefore α should increase during the ^{14}C incubation), this might indicate that
14 the energy transfer efficiency from photochemistry to biomass build-up was much higher in
15 phytoplankton compared to sea ice algae under light limitation (Schuback et al. 2016,
16 Schuback et al. 2017). It should be noted, however, that no spectral correction was applied,
17 and therefore the incubator light could be different between the two methods. While this may
18 affect direct comparison of these two measurements and prevents us from calculating
19 conversion factors, it still allows a comparison between samples from the two habitats. This
20 suggests that in sea ice algae, a substantial fraction of the photosynthetic energy was used for
21 alternative electron sinks (Schuback et al. 2017), possibly an adaption to deal with the
22 extreme environmental conditions within sea ice. These alternative electron sinks could
23 include nutrient assimilation (Laws 1991), carbon concentrating mechanisms (Giordano et al.
24 2005), photorespiration (Foyer et al. 2009), and cyclic electron flow through PSI (Miyake &
25 Asada 2003). In summary, natural phytoplankton assemblages exhibited overall higher

1 electron transport and carbon assimilation rates during the incubation underneath the sea ice
2 compared to sea ice algae (Fig. 7a,b). These results are in line with recent experimental
3 findings confirming that a dominant pelagic diatom was better at taking advantage of
4 increasing irradiances than a sea ice one (Kvernvik et al. 2020).

5

6 4.4. Underlying reasons for the differences between sea ice algae and phytoplankton

7 As outlined above, the field observations and the *in situ* incubation experiment proved that
8 phytoplankton exhibited higher plasticity towards increasing irradiances, had higher carbon
9 fixation rates (both in low and high light) and were less affected by low NO_3^- levels,
10 compared to sea ice algae which exhibited much lower F_v/F_m under high light and low nitrate
11 levels (Fig. 4a). It is important to consider that temporal developments in the taxonomic
12 composition may contribute to changes in photophysiological parameters (Moore et al. 2006,
13 Suggett et al. 2009). Variations in F_v/F_m and σ_{PSII} that could be attributed to phytoplankton
14 community structure were also seen in the current study (Fig. S1). The sea ice algal
15 assemblages were much more homogenous (i.e. strongly dominated by pennate diatoms
16 between stations and dates), whereas the phytoplankton communities were more heterogenous
17 (i.e. mixed and variable dominance of groups) as well as more variable in space and time (Fig.
18 3b). This could be partially explained by the fact that taxonomic changes within highly
19 diverse phytoplankton communities allow for more efficient selection of genotypes that are
20 better adapted to the prevailing light and nutrient environment (Cullen & MacIntyre 1998,
21 Hoppe et al. 2017, Godhe & Rynearson 2017), while the resupply of new genotypes is
22 restricted in the sea ice realm, potentially causing generally lower diversity. For example, the
23 majority of the phytoplankton communities underneath the sea ice (stations MS and Vmf2
24 between 23rd of April and 2nd of May) and at deeper depths in June (25 and 50 meters on 13th
25 of June at Vmf4) was numerically dominated by flagellated cells (mostly *Phaeocystis*

1 *pouchetii* but also dinoflagellates and cryptophytes; > 60 %) while diatoms played a smaller
2 role (< 40%). This is in accordance with previous studies showing that the genus *Phaeocystis*
3 is particularly well adapted to low light environments (Sakshaug & Skjoldal 1989, Moisan et
4 al. 1999, Assmy et al. 2017, Lacour et al. 2017). In June at station Vmf4, surface layers were
5 influenced by meltwater runoff, and as a result the phytoplankton community was numerically
6 dominated (~50 %) by a mixotrophic genus typically occurring in brackish waters, namely
7 *Olisthodiscus* sp. (Hulburt 1965). In August, when nitrate levels were depleted, the majority of
8 the phytoplankton community consisted of mixotrophic species (especially dinoflagellates and
9 cryptophytes) that have differences in energy acquisition strategies (autotrophy vs.
10 mixotrophy; McKie-Krisberg & Saunders 2014). Changes in photophysiological parameters
11 in phytoplankton communities in this study may therefore be due to both differences in
12 antenna structure among dominant taxa and intracellular pigment packaging which generally
13 increase with cell size (Moore et al. 2006, Suggett et al. 2009). Given the subtle to absent
14 effects of environmental differences on photophysiology and stoichiometry of phytoplankton
15 assemblages however, variations in inter- and intraspecific composition seems to provide
16 functional redundancy (i.e. multiple species that perform similar roles in an ecosystem) as
17 previously observed for Arctic phytoplankton (Hoppe et al. 2018a, Wolf et al. 2018). Despite
18 such underlying dynamics, however, we see clear differences in the acclimation potential of
19 sea ice algal and phytoplankton communities that align well with specific physiology of key
20 species of their habitats (e.g. Kvernvik et al. 2020) as well as the environmental conditions
21 they have adapted to. At first glance, it might seem surprising that phytoplankton exhibited
22 higher carbon fixation rates under low irradiance levels compared to sea ice algae during the
23 main bloom period in both habitats (evident from the *in situ* incubation experiment),
24 especially when sea ice algal production typically peaks in early spring when phytoplankton
25 production is very low. However, large scale phytoplankton blooms have recently been

1 observed beneath the sea ice (Mundy et al. 2014, Assmy et al. 2017, Ardyna et al. 2020),
2 where irradiance levels are even lower (both due to absorption by sea ice algae and water)
3 than at the ice-water interface. Also, measurable rates of net primary production in Arctic
4 phytoplankton assemblages at light levels as low as $0.5 \mu\text{mol photons m}^{-2} \text{s}^{-1}$ have recently
5 been observed, indicating that phytoplankton communities can retain net productivity under
6 more extreme low light conditions than previously thought (Kvernvik et al. 2018). We thus
7 speculate that because sea ice algae are adapted to extreme conditions of reduced temperature,
8 high salinities and extremely variable nutrient and inorganic carbon levels, they allocate more
9 of the photosynthetic resources (such as ATP and NADPH) for associated cellular processes
10 (e.g. cryoprotection, osmoregulation, nutrient transport, carbon concentrating mechanisms) so
11 that less of the energy is ending up in the Calvin Cycle and subsequent biomass build-up
12 (Behrenfeld et al. 2008). In fact, Goldman et al. (2014) have suggested that high levels of
13 cyclic electron flow may be a characteristic of psychrophilic phytoplankton that allows them
14 to account for the associated high ATP demand. Since sea ice algae live in more extreme low
15 temperature regimes than phytoplankton, such alternative pathways for electrons could
16 explain the overall lower carbon fixation rates in the former (Fig. 7b). Furthermore, while sea
17 ice algae showed strong signs of high light stress when average daily irradiance levels
18 increased to $> 8 \mu\text{mol photons m}^{-2} \text{s}^{-1}$, the phytoplankton communities were generally light
19 limited within the same irradiance ranges. This could be explained by adaption to strongly
20 contrasting irradiance regimes normally encountered by the two algal assemblages. Reported
21 transmittance through ice and snow layers in the Arctic are often very low (Leu et al. 2010,
22 Leu et al. 2015, Campbell et al. 2016, Assmy et al. 2017, Hancke et al. 2018), and since sea
23 ice algae live in a spatially restricted environment that is normally not undergoing rapid
24 changes, they usually experience gradually changing irradiances of low amplitudes. In
25 comparison, vertical mixing of phytoplankton cells within deeply mixed surface layers goes

1 along with strong and rapid fluctuations in irradiance levels (MacIntyre et al. 2000). For
2 example, phytoplankton in open water in Van Mijenfjorden on the 21st of April 2017 could
3 experience irradiance levels ranging from 0 to 100 $\mu\text{mol photons m}^{-2} \text{ s}^{-1}$, due to vertical
4 movement within a mixed layer depth of 20 m (estimated from the thermocline at Vmf1). In
5 comparison, irradiance levels at the ice-water interface the same day ranged between 0.1 and
6 0.8 $\mu\text{mol photons m}^{-2} \text{ s}^{-1}$ (Fig. 8a,b). Hence, it is expedient for phytoplankton to evolve
7 pronounced mechanisms for dealing with highly dynamic irradiance conditions (e.g.
8 Behrenfeld et al. 1998, White et al. 2020). This is also true for periodically ice-covered
9 system such as Arctic fjords, where strong wind events can push the land fast ice out of the
10 fjord over short time spans. This is in line with the fact that Arctic phytoplankton assemblages
11 have also been shown to be rather resistant to changes in temperature, irradiance and $p\text{CO}_2$, a
12 finding that has been explained by the high environmental variability they have to cope with
13 (Hoppe et al. 2018b).

14 It hence seems that both physiological acclimation to variable irradiance and nutrient levels
15 and taxonomic composition must be considered when assessing photosynthetic performance
16 in algal assemblages. The results from this study imply major differences in energy allocation
17 between sea ice algae and phytoplankton when exposed to high light and low nutrients. sea
18 ice algae seem to allocate more energy into photoprotective mechanisms and alternative
19 energy sinks (e.g. NPQ, photorespiration, Mehler reaction, cyclic electron transport through
20 PSI), that may allow optimization of cellular processes for tolerating extreme environmental
21 conditions but result in lower rates of linear electron transport and carbon assimilation. In
22 phytoplankton, taxonomic and functional changes, as well as high photoacclimative capacity
23 of these taxa together with higher probability of nutrients resupply were probably the
24 underlying reasons for the subtle or absent trends in photophysiology and biochemical
25 responses, but in return ensured high rates of photosynthesis under a wide range of irradiance

1 and NO_3^- levels. It seems that the contrasting environmental conditions in polar seas and sea
2 ice may have led to such specific adaptations and acclimation strategies.

3

4 **5. Conclusion**

5 Knowledge of physiological and biochemical responses of sea ice algae and phytoplankton
6 towards their changing environment is essential to understand how the balance between sea
7 ice-based vs. pelagic primary production will change with respect to timing and quantity in a
8 future Arctic. The results from this study suggest that sea ice algae will be more sensitive than
9 phytoplankton towards the expected environmental changes, in particular increased
10 irradiance. Our findings also clearly highlight the importance of considering interactive
11 effects of environmental variables, as well as the value of comparing functionally distinct
12 communities to gain a mechanistic understanding of response patterns. The contribution of
13 more diverse phytoplankton assemblages, with their high plasticity and potential for
14 functional redundancy, to annual primary production in the Arctic will likely increase, based
15 on the ability of phytoplankton to take advantage of higher irradiances in a habitat that is
16 becoming more prevalent in the future. For sea ice algae, on the contrary, we can probably
17 anticipate a decrease in their relative contribution to annual primary production, not only
18 because sea ice cover is generally declining but also because the remaining sea ice is getting
19 thinner and transmits more light, a situation for which our data indicate reduced
20 photosynthetic performance of sea ice algae. These findings may be especially relevant as the
21 importance of ephemeral sea ice (i.e. melting and re-forming) is likely to increase in the future
22 (Onarheim et al. 2018). Hence, organisms inhabiting the sea ice will have to deal with much
23 more dynamic environmental settings, and with ongoing climate change, characteristic sea ice
24 algae species might be outcompeted by less sensitive species, thereby potentially altering the
25 algal colonization of young Arctic sea ice. This could have important implications for trophic

1 interactions, carbon fluxes and budgets. Hence, an improved and differentiated
2 parametrization of primary production derived from sea ice algae vs. phytoplankton is
3 urgently required in modeling contexts, and needs to include important functional differences
4 of these algal communities as described here.

5

6 **Acknowledgements**

7 This study was funded by the Norwegian Research Council as part of the project FAABulous:
8 Future Arctic Algae Blooms – and their role in the context of climate change (project nr.
9 243702) and partly financed by Polish Ministry of Science and Higher Education (MNiSW).
10 Laura Wischnewski, Marcel Machnik and Benoit Lebreton are acknowledged for their help
11 with nutrient and organic matter composition sample analyses. Marcel Nicolaus and Martin
12 Schiller are acknowledged for the deployment of SIMBA and snow buoy, Dirk Notz and Leif
13 Riemenschneider for the irradiance logger data.

14

15 **References**

- 16 Alou-Font E, Mundy CJ, Roy S, Gosselin M, Agustí S (2013) Snow cover affects ice algal
17 pigment composition in the coastal Arctic ocean during spring. *Mar Ecol Prog Ser*
18 474:89-104.
- 19 Ardyna M, Arrigo KR (2020) Phytoplankton dynamics in a changing Arctic Ocean. *Nature*
20 *Climate Change* 10:892-903.
- 21 Ardyna M, Mundy CJ, Mayot N, Matthes LC, Oziel L, Horvat C, Leu E, Assmy P, Hill V,
22 Matrai PA, Gale M, Melnikov IA, Arrigo KR (2020) Under-Ice Phytoplankton
23 Blooms: Shedding Light on the “Invisible” Part of Arctic Primary Production. *Front*
24 *Mar Sci* 7:608032. Doi: 10.3389/fmars.2020.608032

- 1 Arrigo KR, Mock T, Lizotte MP (2010) Primary producers and sea ice. In: Thomas DN,
2 Dieckmann GS (eds). Sea ice 2nd edition. Wiley-Blackwell, Oxford, UK, p 283-325
- 3 Arrigo KR, Perovich DK, Pickart RS, Brown ZW, Van Dijken GL, Lowry KE, Mills MM,
4 Palmer MA, Balch WM, Bahr F (2012) Massive phytoplankton blooms under Arctic
5 sea ice. Science 1215065. Doi: 10.1126/science.1215065
- 6 Arrigo KR, Brown ZW, Mills MM (2014) Sea ice algal biomass and physiology in the
7 Amundsen Sea, Antarctica. Elem Sci Anth 2:p.000028.
8 Doi: 10.12952/journal.elementa.000028
- 9 Assmy P, Fernández-Méndez M, Duarte P, Meyer A, Randelhoff A, Mundy CJ, Olsen LM,
10 Kauko HM, Bailey A, Chierici M (2017) Leads in Arctic pack ice enable early
11 phytoplankton blooms below snow-covered sea ice. Sci Rep 7:40850.
12 Doi: 10.1038/srep40850
- 13 Aumack C, Juhl A (2015) Light and nutrient effects on the settling characteristics of the sea
14 ice diatom *Nitzschia frigida*. Limnol Oceanogr 60:765-776.
- 15 Barlow R, Gosselin M, Legendre L, Therriault JC, Demers S, Mantoura R, Llewellyn C
16 (1988) Photoadaptive strategies in sea-ice microalgae. Mar Ecol Prog Ser 45:145-152.
- 17 Bates SS, Cota GF (1986) Fluorescence induction and photosynthetic responses of Arctic ice
18 algae to sample treatment and salinity. J Phycol 22:421-429.
- 19 Behrenfeld MJ, Prasil O, Kolber ZS, Babin M, Falkowski PG (1998) Compensatory changes
20 in photosystem II electron turnover rates protect photosynthesis from photoinhibition.
21 Photosynth Res 58:259-268
- 22 Behrenfeld MJ, Halsey KH, Milligan AJ (2008) Evolved physiological responses of
23 phytoplankton to their integrated growth environment. Phil Trans R Soc, B: Biological
24 Science 363:2687-2703.
- 25 Brunet C, Johnsen G, Lavaud J, Roy S (2011) Pigments and photoacclimation processes. In:

- 1 Roy S, Llewellyn CA, Egeland ES and Johnsens G (eds). Phytoplankton pigments:
2 Characterization, Chemotaxonomy and Applications in Oceanography. Cambridge
3 university press, UK p 445-454
- 4 Campbell K, Mundy C, Landy J, Delaforge A, Michel C, Rysgaard S (2016) Community
5 dynamics of bottom-ice algae in Dease Strait of the Canadian Arctic. *Prog Oceanogr*
6 149:27-39
- 7 Carmack E, Wassmann P (2006) Food webs and physical–biological coupling on pan-Arctic
8 shelves: unifying concepts and comprehensive perspectives. *Prog Oceanogr* 71:446-
9 477.
- 10 Coello-Camba A, Agustí S, Vaqué D, Holding J, Arrieta JM, Wassmann P, Duarte CM (2015)
11 Experimental assessment of temperature thresholds for Arctic phytoplankton
12 communities. *Estuar Coasts* 38:873-885
- 13 Cosgrove J, Borowitzka MA (2010) Chlorophyll Fluorescence Terminology: An
14 Introduction. In: Suggett D, Prášil O, Borowitzka M (eds) *Chlorophyll a*
15 *Fluorescence in Aquatic Sciences: Methods and Applications*. Developments in
16 *Applied Phycology*, vol 4. Springer, Dordrecht. Doi: /10.1007/978-90-481-9268-
17 7_1
- 18 Cota GF (1985) Photoadaptation of high Arctic ice algae. *Nature* 315:219-222
- 19 Cota GF, Legendre L, Gosselin M, Ingram R (1991) Ecology of bottom ice algae: I.
20 Environmental controls and variability. *J Mar Syst* 2:257-277
- 21 Cox G, Weeks W (1986) Changes in the salinity and porosity of sea-ice samples during
22 shipping and storage. *J Glaciol* 32:371-375
- 23 Cullen JJ, MacIntyre JG (1998) Behavior, physiology and the niche of depth-regulating
24 phytoplankton. *NATO Adv Sci I G-Eco* 41:559-580

1 Daase M, Falk-Petersen S, Varpe Ø, Darnis G, Søreide JE, Wold A, Leu E, Berge J, Philippe
2 B, Fortier L (2013) Timing of reproductive events in the marine copepod *Calanus*
3 *glacialis*: a pan-Arctic perspective. *Can J Fish Aquat Sci* 70:871-884

4 Danielson SL, Eisner L, Ladd C, Mordy C, Sousa L, Weingartner TJ (2017) A comparison
5 between late summer 2012 and 2013 water masses, macronutrients, and phytoplankton
6 standing crops in the northern Bering and Chukchi Seas. *Deep Sea Res II* 135:7-26

7 Demers S, Legendre L, Maestrini SY, Rochet M, Ingram RG (1989) Nitrogenous nutrition of
8 sea-ice microalgae. *Polar Biol* 9:377-383

9 Eberhard S, Finazzi G, Wollman F-A (2008) The dynamics of photosynthesis. *Annu Rev*
10 *Genet* 42:463-515

11 Eilers P, Peeters J (1988) A model for the relationship between light intensity and the rate of
12 photosynthesis in phytoplankton. *Ecological modelling* 42:199-215

13 Foyer CH, Bloom AJ, Queval G, Noctor G (2009) Photorespiratory metabolism: genes,
14 mutants, energetics, and redox signaling. *Annu Rev of Plant Biol* 60:455-484

15 Frigstad H, Andersen T, Bellerby RG, Silyakova A, Hessen DO (2014) Variation in the seston
16 C: N ratio of the Arctic Ocean and pan-Arctic shelves. *J Mar Syst* 129:214-223

17 Galindo V, Gosselin M, Lavaud J, Mundy CJ, Else B, Ehn J, Babin M, Rysgaard S (2017)
18 Pigment composition and photoprotection of Arctic sea ice algae during spring. *Mar*
19 *Ecol Prog Ser* 585:49-69

20 Garrison DL, Buck KR (1986) Organism losses during ice melting: a serious bias in sea ice
21 community studies. *Polar Biol* 6:237-239

22 Geider RJ, La Roche J, Greene RM, Olaizola M (1993) Response of the photosynthetic
23 apparatus of *Phaeodactylum tricornutum* (Bacillariophyceae) to nitrate, phosphate, or
24 iron starvation. *J Phycol* 29:755-766

- 1 Giordano M, Beardall J, Raven JA (2005) CO₂ concentrating mechanisms in algae:
2 mechanisms, environmental modulation, and evolution. *Annu Rev Plant Biol* 56:99-
3 131
- 4 Godhe A, Rynearson T (2017) The role of intraspecific variation in the ecological and
5 evolutionary success of diatoms in changing environments. *Phil Trans R Soc B* 372:
6 20160399. Doi: 10.1098/rstb.2016.0399
- 7 Goldman JA, Kranz SA, Young JN, Tortell PD, Stanly RH, Bender ML, Morel FM (2014)
8 Gross and net production during the spring bloom along the Western Antarctic
9 Peninsula. *New Phytol* 205: 182-191
- 10 Gosselin M, Legendre L, Therriault JC, Demers SJ (1990) Light and nutrient limitation of
11 sea-ice microalgae (Hudson bay, Canadian Arctic). *J Phycol* 26:220-232
- 12 Gosselin M, Levasseur M, Wheeler PA, Horner RA, Booth BC (1997) New measurements of
13 phytoplankton and ice algal production in the Arctic Ocean. *Deep Sea Res II* 44:1623-
14 1644
- 15 Hancke K, Lund-Hansen LC, Lamare ML, Højlund Pedersen S, King MD, Andersen P,
16 Sorrell BK (2018) Extreme low light requirement for algae growth underneath sea ice:
17 A case study from station nord, NE Greenland. *J Geophys Res: Oceans* 123:985-1000
- 18 Hansell DA, Whitledge TE, Goering JJ (1993) Patterns of nitrate utilization and new
19 production over the Bering-Chukchi shelf. *Cont Shelf Res* 13:601-627
- 20 Hegseth EN, Sundfjord A (2008) Intrusion and blooming of Atlantic phytoplankton species in
21 the high Arctic. *J Mar Syst* 74:108-119
- 22 Henley SF, Porter M, Hobbs L, Braun J, Guillaume-Castel R, Venables EJ, Dumont E, Cottier
23 F (2020) Nitrate supply and uptake in the Atlantic Arctic sea ice zone: seasonal cycle,
24 mechanisms and drivers. *Phil Trans R Soc A* 378:20190361.
25 Doi: 10.1098/rsta.2019.0361

1 Hill V, Cota G (2005) Spatial patterns of primary production on the shelf, slope and basin of
2 the Western Arctic in 2002. *Deep Sea Res II* 52:3344-3354

3 Hill VJ, Light B, Steele M, Zimmerman RC (2018) Light availability and phytoplankton
4 growth beneath Arctic sea ice: Integrating observations and modeling. *J Geophys Res:*
5 *Oceans* 123:3651-3667

6 Holm-Hansen O, Riemann B (1978) Chlorophyll a determination: improvements in
7 methodology. *Oikos*:438-447

8 Hoppe CJM, Holtz LM, Trimborn S, Rost B (2015) Ocean acidification decreases the light-
9 use efficiency in an Antarctic diatom under dynamic but not constant light. *New*
10 *Phytol* 207:159-171

11 Hoppe CJM, Schuback N, Semeniuk D, Maldonado MT, Rost B (2017) Functional
12 redundancy mediates phytoplankton resilience to ocean acidification and increased
13 irradiances. *Frontiers in Marine Science*, 4:229. Doi: 10.3389/fmars.2017.00229

14 Hoppe CJM, Schuback N, Semeniuk D, Giesbrecht K, Mol J, Thomas H, Maldonado M, Rost
15 B, Varela D, Tortell P (2018a) Resistance of Arctic phytoplankton to ocean
16 acidification and enhanced irradiance. *Polar Biol* 41:399-413

17 Hoppe CJM, Wolf KK, Schuback N, Tortell PD, Rost B (2018b) Compensation of ocean
18 acidification effects in Arctic phytoplankton assemblages. *Nat Clim Change* 8:529-
19 533

20 Hoppe CJM, Wischniewski L, Leu E, Brown T, Graeve M, Wiktor JM, Verbiest S, Kvernvik
21 AC (2020) Inorganic nutrients measured on water bottle samples from CTD Water-
22 sampler system and ice cores during FAABulous project period (2015-2018). Alfred
23 Wegenes Institute, Helmholtz centre for polar and marine research, Bremerhaven,
24 PANGEA. Doi: <https://doi.pangaea.de/10.1594/PANGAEA.925007> (dataset in
25 review)

1 Hulburt EM (1965) Flagellates from brackish waters in the vicinity of Woods Hole,
2 Massachusetts. *J phycol* 1:87-94

3 Huntington HP, Danielson SL, Wiese FK, Baker M, Boveng P, Citta JJ, De Robertis A,
4 Dickson DM, Farley E, George JC (2020) Evidence suggests potential transformation
5 of the Pacific Arctic ecosystem is underway. *Nature Climate Change* 10:342-348

6 Høyland KV (2009) Ice thickness, growth and salinity in Van Mijenfjorden, Svalbard,
7 Norway. *Polar Res* 28:339-352

8 Johnsen G, Norli M, Moline M, Robbins I, von Quillfeldt C, Sørensen K, Cottier F, Berge J
9 (2018) The advective origin of an under-ice spring bloom in the Arctic Ocean using
10 multiple observational platforms. *Polar Biol* 41:1197-1216

11 Juhl AR, Krembs C (2010) Effects of snow removal and algal photoacclimation on growth
12 and export of ice algae. *Polar Biol* 33:1057-1065

13 Kangas T (2000) Thermohaline sesongvariasjoner i Van Mijenfjorden. MSc thesis, University
14 of Bergen, Norway.

15 Kiefer D (1973) Chlorophyll a fluorescence in marine centric diatoms: responses of
16 chloroplasts to light and nutrient stress. *Mar Biol* 23:39-46

17 Kirst GO, Wiencke C (1995) Ecophysiology of polar algae. *J Phycol* 31:181-199

18 Krause G, Weis E (1991) Chlorophyll fluorescence and photosynthesis: the basics. *Annu Rev*
19 *Plant Biol* 42:313-349

20 Kulk G, van de Poll WH, Buma AGJ (2018) Photophysiology of nitrate limited
21 phytoplankton communities in Kongsfjorden, Spitsbergen. *Limnol Oceanogr* 63:2606-
22 2617

23 Kvernvik AC, Hoppe CJM, Lawrenz E, Prášil O, Greenacre M, Wiktor JM, Leu E (2018) Fast
24 reactivation of photosynthesis in arctic phytoplankton during the polar night. *J Phycol*
25 54:461-470

- 1 Kvernvik AC, Rokitta SD, Leu E, Harms L, Gabrielsen TM, Rost B, Hoppe CJM (2020)
2 Higher sensitivity towards light stress and ocean acidification in an Arctic
3 sea.ice.associated diatom compared to a pelagic diatom. *New phytol* 226:1708-1724
- 4 Kwok R, Cunningham G, Wensnahan M, Rigor I, Zwally H, Yi D (2009) Thinning and
5 volume loss of the Arctic Ocean sea ice cover: 2003–2008. *J Geophys Res: Oceans*
6 114:C07005. Doi: 10.1029/2009JC005312
- 7 Lacour T, Larivière J, Babin M (2017) Growth, Chl a content, photosynthesis, and elemental
8 composition in polar and temperate microalgae. *Limnol Oceanogr* 62:43-58
- 9 Lacour T, Babin M, Lavaud J (2020) Diversity in xanthophyll cycle pigments content and
10 related Nonphotochemical Quenching (NPQ) among microalgae: Implications for
11 growth strategy and ecology. *J Phycol* 56:245-263
- 12 Laws EA (1991) Photosynthetic quotients, new production and net community production in
13 the open ocean. *Deep-sea Res A, Oceanogr Res Pap* 38:143-167
- 14 Legendre L, Ackley SF, Dieckmann GS, Gulliksen B, Horner R, Hoshiai T, Melnikov IA,
15 Reeburgh WS, Spindler M, Sullivan CW (1992) Ecology of sea ice biota. *Polar Biol*
16 12:429-444
- 17 Leppäranta M, Manninen T (1988) The brine and gas content of sea ice with attention to low
18 salinities and high temperatures. Internal Rep 88-2, Finn Inst Mar Res, Helsinki,
19 Finland
- 20 Leu E, Wängberg S-Å, Wulff A, Falk-Petersen S, Ørbæk JB, Hessen DO (2006) Effects of
21 changes in ambient PAR and UV radiation on the nutritional quality of an Arctic
22 diatom (*Thalassiosira antarctica* var. *borealis*). *J Exp Mar Biol Ecol* 337:65-81
- 23 Leu E, Wiktor J, Søreide J, Berge J, Falk-Petersen S (2010) Increased irradiance reduces food
24 quality of sea ice algae. *Mar Ecol Prog Ser* 411:49-60

- 1 Leu E, Mundy C, Assmy P, Campbell K, Gabrielsen T, Gosselin M, Juul-Pedersen T,
2 Gradinger R (2015) Arctic spring awakening—Steering principles behind the
3 phenology of vernal ice algal blooms. *Prog Oceanogr* 139:151-170
- 4 Leu E, Schiller M, Nicolaus M (2018) Snow height on sea ice and sea ice drift from
5 autonomous measurements from buoy 2017S43, deployed during FAABulous 2017.
6 Alfred Wegener Institute, Helmholtz centre for polar and marine research,
7 Bremerhaven, PANGEA. Doi: 10.1594/PANGEA.887811
- 8 Leu E, Brown TA, Graeve M, Wiktor J, Hoppe CJM, Chierici M, Fransson A, Verbiest S,
9 Kvernvik AC, Greenacre MJ (2020) Spatial and temporal variability of ice algal
10 trophic markers – with recommendations about their application. *J Mar Sci Eng* 8:676.
11 Doi: 10.3390/jmse8090676
- 12 Lewis K, Arntsen A, Coupel P, Joy- Warren H, Lowry K, Matsuoka A, Mills M, van Dijken
13 G, Selz V, Arrigo K (2018) Photoacclimation of Arctic Ocean phytoplankton to
14 shifting light and nutrient limitation. *Limnol Oceanogr* 9999:1-18
- 15 Litchman E, Klausmeier CA (2008) Trait-based community ecology of phytoplankton. *Annu*
16 *Rev Ecol Evol Syst* 39:615-639
- 17 Litchman E, Neale PJ, Banaszak AT (2002) Increased sensitivity to ultraviolet radiation in
18 nitrogen-limited dinoflagellates: photoprotection and repair. *Limnol Oceanogr* 47:86-
19 94
- 20 Loose B, Miller LA, Elliott S, Papakyriakou T (2011) Sea ice biogeochemistry and material
21 transport across the frozen interface. *Oceanogr* 24:202-218
- 22 MacIntyre HL, Kana TM, Geider RJ (2000) The effect of water motion on short-term rates of
23 photosynthesis by marine phytoplankton. *Trends Plant Sci* 5:12-17

- 1 Marks AA, King MD (2014) The effect of snow/sea ice type on the response of albedo and
2 light penetration depth (e-folding depth) to increasing black carbon. *The cryosphere*
3 8:1625-1638
- 4 McKie-Krisberg ZM, Sanders RW (2014) Phagotrophy by the picoeukaryotic green alga
5 *Micromonas*: implications for Arctic Oceans. *ISME J* 8:1953-1961
- 6 McMinn A, Müller MN, Martin A, Ryan KG (2014) The response of Antarctic sea ice algae
7 to changes in pH and CO₂. *PLOS ONE* 9:e86984. Doi: 10.1371/journal.pone.0086984
- 8 Miyake C, Asada K (2003) The water-water cycle in algae. In: Larkum AWD, Douglas SE,
9 Raven JA (eds) *Photosynthesis in Algae. Advances in photosynthesis and respiration*
10 vol 14. Springer, Dordrecht, Netherland p 183-204
- 11 Moisan TA, Mitchell BG (1999) Photophysiological acclimation of *Phaeocystis antarctica*
12 Karsten under light limitation. *Limnol Oceanogr* 44:247-258
- 13 Moore CM, Suggett DJ, Hickman AE, Kim Y-N, Tweddle JF, Sharples J, Geider RJ, Holligan
14 PM (2006) Phytoplankton photoacclimation and photoadaptation in response to
15 environmental gradients in a shelf sea. *Limnol Oceanogr* 51:936-949
- 16 Mundy CJ, Barber D, Michel C (2005) Variability of snow and ice thermal, physical and
17 optical properties pertinent to sea ice algae biomass during spring. *J Mar Syst* 58:107-
18 120
- 19 Mundy CJ, Gosselin M, Gratton Y, Brown K, Galindo V, Campbell K, Levasseur M, Barber
20 D, Papakyriakou T, Bélanger S (2014) Role of environmental factors on
21 phytoplankton bloom initiation under landfast sea ice in Resolute Passage, Canada.
22 *Mar Ecol Prog Ser* 497:39-49
- 23 Nicolaus M, Katlein C, Maslanik J, Hendricks S (2012) Changes in Arctic sea ice result in
24 increasing light transmittance and absorption. *Geophys Res Lett* 39: L24501. Doi:
25 10.1029/2012GL053738

1 Niemi A, Michel C (2015) Temporal and spatial variability in sea-ice carbon: nitrogen ratios
2 on Canadian Arctic shelves. *Elem sci Anth* 3: p.000078. Doi:
3 10.12952/journal.elementa.000078

4 Nöthig E-M, Bracher A, Engel A, Metfies K, Niehoff B, Peeken I, Bauerfeind E, Cherkasheva
5 A, Gäbler-Schwarz S, Hardge K, Kiliyas E, Kraft A, Mebrahtom K, Lalande C,
6 Piontek J, Thomisch K, Wurst M (2015) Summertime plankton ecology in Fram
7 Strait—a compilation of long- and short-term observations. *Polar Research* 34:1,
8 23349. Doi: 10.3402/polar.v34.23349

9 Onarheim IH, Eldevik T, Smedsrud LH, Stroeve JC (2018) Seasonal and regional
10 manifestation of Arctic sea ice loss. *J Clim* 31:4817-4932

11 Oxborough K (2012) FastPro8 GUI and FRRf3 systems documentation. West Molesey, UK:
12 Chelsea Technologies Group Ltd

13 Perrette M, Yool A, Quartly G, Popova E (2011) Near-ubiquity of ice-edge blooms in the
14 Arctic. *Biogeosci* 8:515-524

15 Peterson BJ, Holmes RM, McClelland JW, Vörösmarty CJ, Lammers RB, Shiklomanov AI,
16 Shiklomanov IA, Rahmstorf S (2002) Increasing river discharge to the Arctic Ocean.
17 *Science* 298:2171-2173

18 Poulin M, Daugbjerg N, Gradinger R, Ilyash L, Ratkova T, von Quillfeldt C (2011) The pan-
19 Arctic biodiversity of marine pelagic and sea-ice unicellular eukaryotes: a first-attempt
20 assessment. *Mar Biodivers* 41:13-28

21 R Core Team (2017) R: A language and environment for statistical computing. Vienna,
22 Austria: R Foundation for Statistical Computing. R Foundation for Statistical
23 Computing, Vienna, Austria. Available at: <https://www.R-project.org/>.

24 Ratkova TN, Wassmann P (2002) Seasonal variation and spatial distribution of phyto- and
25 protozooplankton in the central Barents Sea. *J Mar Syst* 38:47-75

- 1 Rodriguez F, Chauton M, Johnsen G, Andresen K, Olsen L, Zapata M (2006)
2 Photoacclimation in phytoplankton: implications for biomass estimates, pigment
3 functionality and chemotaxonomy. *Mar Biol* 148:963-971
- 4 Rousseau V, Mathot S, Lancelot C (1990) Calculating carbon biomass of *Phaeocystis* sp.
5 from microscopic observations. *Mar Biol* 107:305-14
- 6 Runge JA, Therriault JC, Legendre L, Ingram RG, Demers S (1991) Coupling between ice
7 microalgal productivity and the pelagic, metazoan food web in southeastern Hudson
8 Bay: a synthesis of results. *Polar Res* 10:325-338
- 9 Sakshaug E (2004) Primary and secondary production in the Arctic seas. In: Stein R,
10 MacDonald RW (eds) *The organic carbon cycle in the Arctic Ocean*. Springer Berlin
11 Heidelberg, Berlin, Heidelberg p 57-81
- 12 Sakshaug E, Skjoldal HR (1989) Life at the ice edge. *Ambio* 18:60-67
- 13 Sakshaug E, Bricaud A, Dandonneau Y, Falkowski PG, Kiefer DA, Legendre L, Morel A,
14 Parslow J, Takahashi M (1997) Parameters of photosynthesis: definitions, theory and
15 interpretation of results. *J Plankton Res* 19:1637-1670
- 16 Schuback N, Flecken M, Maldonado MT, Tortell PD (2016) Diurnal variation in the coupling
17 of photosynthetic electron transport and carbon fixation in iron-limited phytoplankton
18 in the NE subarctic Pacific. *Biogeosci* 13:1019-1035
- 19 Schuback N, Hoppe CJM, Tremblay J-É, Maldonado MT, Tortell PD (2017) Primary
20 productivity and the coupling of photosynthetic electron transport and carbon fixation
21 in the Arctic Ocean. *Limnol Oceanogr* 62:898-921
- 22 Screen JA, Simmonds I (2012) Declining summer snowfall in the Arctic: causes, impacts and
23 feedbacks. *Clim Dyn* 38:2243-2256

- 1 Screen JA, Simmonds I, Keay K (2011) Dramatic interannual changes of perennial Arctic sea
2 ice linked to abnormal summer storm activity. *J Geophys Res: Atmospheres*
3 116_D15105. Doi: 10.1029/2011JD015847
- 4 Sterner R, Elser JJ (2002) *Ecological stoichiometry: The biology of elements from molecules*
5 *to the biosphere*. Princeton University Press, Oxford, UK, p 464
- 6 Strom SL, Olson MB, Macri EL, Mordy CW (2006) Cross-shelf gradients in phytoplankton
7 community structure, nutrient utilization, and growth rate in the coastal Gulf of
8 Alaska. *Mar Ecol Prog Ser* 328:75-92
- 9 Suggett DJ, Moore CM, Hickman AE, Geider RJ (2009) Interpretation of fast repetition rate
10 (FRR) fluorescence: signatures of phytoplankton community structure versus
11 physiological state. *Mar Ecol Prog Ser* 376:1-19
- 12 Swinehart DJ (1962) The beer-lambert law. *J Chem Educ* 39:333-335
- 13 Søreide JE, Hop H, Carroll ML, Falk-Petersen S, Hegseth EN (2006) Seasonal food web
14 structures and sympagic–pelagic coupling in the European Arctic revealed by stable
15 isotopes and a two-source food web model. *Prog Oceanogr* 71:59-87
- 16 Søreide JE, Leu E, Berge J, Graeve M, Falk- Petersen S (2010) Timing of blooms, algal food
17 quality and *Calanus glacialis* reproduction and growth in a changing Arctic. *Glob*
18 *Change Biol* 16:3154-3163
- 19 Torstensson A, Dinasquet J, Chierici M, Fransson A, Riemann L, Wulff A (2015)
20 Physicochemical control of bacterial and protist community composition and diversity
21 in Antarctic sea ice. *Environ Microbiol* 17:3869-3881
- 22 Tremblay JÉ, Gagnon J (2009) The effects of irradiance and nutrient supply on the
23 productivity of Arctic waters: a perspective on climate change. In: Nihoul JCJ,
24 Kostianoy AG (eds) *Influence of Climate Change on the Changing Arctic and Sub-*
25 *Arctic Conditions*. NATO Sci Peace Sec C, Springer, Dordrecht Netherlands p 73-93

- 1 Utermöhl H (1958) Zur Vervollkommnung der quantitativen Phytoplankton-Methodik. Mitt
2 Int Ver Theor Angew Limnol, Stuttgart, Germany, p 38
- 3 Van De Poll WH, Van Leeuwe MA, Roggeveld J, Buma AG (2005) Nutrient limitation and
4 high irradiance acclimation reduce PAR and UV-induced viability loss in the Antarctic
5 diatom *Chaetoceros Brevis* (Bacillariophyceae). J Phycol 41:840-850
- 6 Van De Poll WH, Maat DS, Fischer P, Rozema PD, Daly OB, Koppelle S, Visser RJW, Buma
7 AGJ (2016) Atlantic Advection Driven Changes in Glacial Meltwater: Effects on
8 Phytoplankton Chlorophyll-a and Taxonomic Composition in Kongsfjorden,
9 Spitsbergen. Frontiers in Marine Science 3:200. Doi: 10.3389/fmars.2016.00200
- 10 Varela DE, Crawford DW, Wrohan IA, Wyatt SN, Carmack EC (2013) Pelagic primary
11 productivity and upper ocean nutrient dynamics across Subarctic and Arctic Seas. J
12 Geophys Res: Oceans 118:7132-7152
- 13 von Quillfeldt CH, Ambrose WG, Clough LM (2003) High number of diatom species in first-
14 year ice from the Chukchi Sea. Polar Biol 26:806-818
- 15 Weeks WF, Ackley SF (1986) The growth, structure, and properties of sea ice. In:
16 Untersteiner N (eds) The geophysics of sea ice. Springer, Boston, US p 9-164
- 17 White E, Hoppe CJM, Rost B (2020) The Arctic picoeukaryote *Micromonas pusilla* benefits
18 from ocean acidification under constant and dynamic light. Biogeosciences 17:635-
19 647
- 20 Willis K, Cottier F, Kwasniewski S, Wold A, Falk-Petersen S (2006) The influence of
21 advection on zooplankton community composition in an Arctic fjord (Kongsfjorden,
22 Svalbard). J Mar Sys 61:39-54
- 23 Wolf KKE, Hoppe CJM, Rost B (2018) Resilience by diversity: Large intraspecific
24 differences in climate change responses of an Arctic diatom. Limnol Oceanogr
25 63:397-411

Accepted Article

1 **Table 1.** Table containing station names, sampling dates, sampled depths (phytoplankton),
2 snow and ice thickness [cm], average daily irradiances [$\mu\text{mol photons m}^{-2} \text{s}^{-1}$], ocean/brine
3 salinity [PSU], ocean/brine temperature [$^{\circ}\text{C}$], NO_3^- levels [$\mu\text{mol L}^{-1}$] as well as Chl a [$\mu\text{g L}^{-1}$]
4 and POC:Chl a [$\mu\text{g C } \mu\text{g Chla}^{-1}$]. At each station sea ice algae and/or phytoplankton were
5 sampled designated by S and P. Asterix (*) designates phytoplankton sampling conducted
6 underneath the sea ice, while the rest was conducted in open water. Na defines “not
7 available”.

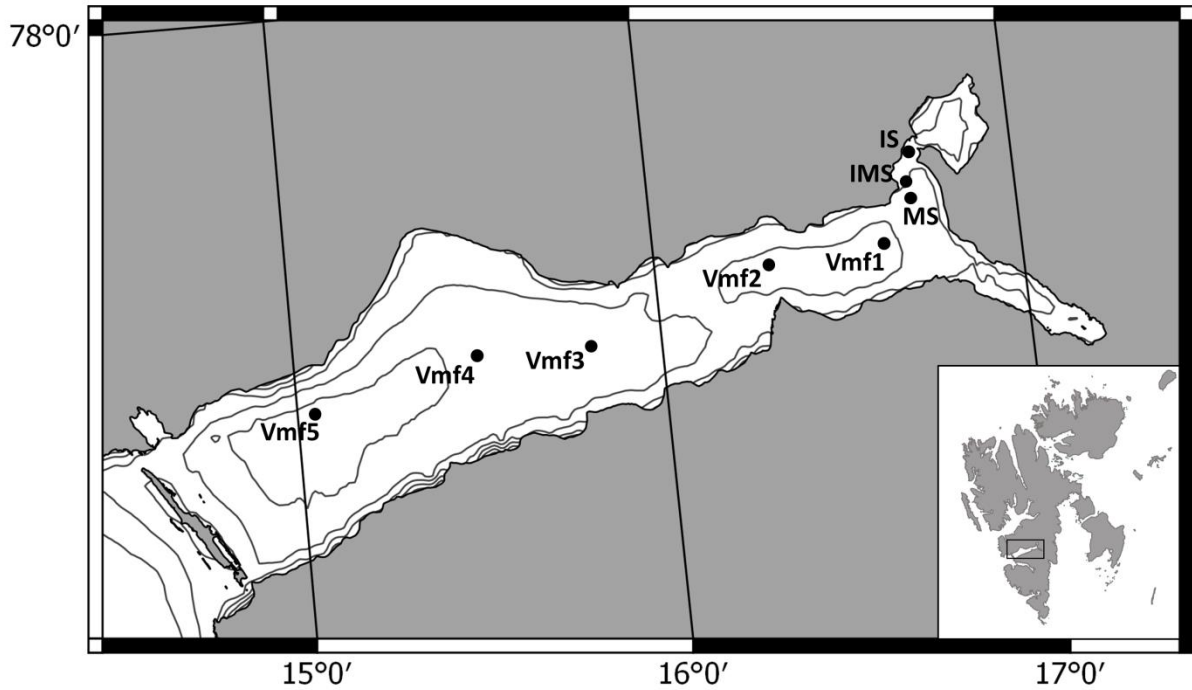
Station	Sea ice algae /Phyto- plankton	Date	Depth [m]	Snow [cm]	Ice [cm]	Irradiance [$\mu\text{mol photons m}^{-2}$ s^{-1}]	Salinity [PSU]	Temp [$^{\circ}\text{C}$]	NO_3^- [$\mu\text{mol L}^{-1}$]	Chl a [$\mu\text{g L}^{-1}$]	POC:Chla [$\mu\text{g C } \mu\text{g Chla}^{-1}$]
IS	S	28.04.17	Na	7-8.5	57	5-6	33.9	-1.9	16.2	190.4	73.4
IM	S	28.04.17	Na	19	55	3	28.7	-1.6	5.2	119.5	43.2
MS	S	09.03.17	Na	8	29	2	35.6	-2	1.42	0.4	Na
MS	S	07.04.17	Na	4-8	49	3-9	28.7	-1.6	3.90	68.8	32.9
MS	S	23.04.17	Na	3-3.5	55	20-22	33.9	-1.9	2.91	252.3	35.3
MS	S	23.04.17	Na	19-20	55	4-5	35.1	-2	14.28	259.2	23.0
MS	S	02.05.17	Na	0	52	74	31.6	-1.8	0.17	106.6	94.6
MS	S	02.05.17	Na	20	52	7	31.4	-1.7	0.67	161.4	47.1
Vmf1	S	07.04.17	Na	5-6	44	5-7	30.5	-1.7	12.41	300.7	20.4
Vmf1	S	30.04.17	Na	15-16	40	10-11	29.8	-1.7	0.49	181.5	53.9
Vmf2	S	26.04.17	Na	3.5-5	40	14-19	35.0	-2	0.75	72.5	57.5
Vmf2	S	26.04.17	Na	26-27	40	3	33.4	-1.8	2.70	58.1	13.5
MS	P*	23.04.17	0	Na	55	12	34.7	-1.8	9.62	0.4	945.3
MS	P*	02.05.17	0	Na	52	40	34.6	-1.6	0.91	5.4	45.9
Vmf1	P*	30.04.17	0	Na	40	11	34.6	-1.7	0.42	14.9	27.7
Vmf1	P	23.08.17	5	Na	Na	1	31.3	5.4	0.00	1.9	141.6
Vmf1	P	23.08.17	25	Na	Na	0	33.4	4.3	0.22	1.9	118.6
Vmf2	P*	26.04.17	0	Na	40	10	34.6	-1.7	1.92	6.5	74.6
Vmf3	P	13.03.17	0	Na	Na	27	34.6	-1.4	10.17	0.1	Na
Vmf3	P	13.03.17	5	Na	Na	13	34.6	-1.4	10.19	0.1	Na
Vmf3	P	13.03.17	25	Na	Na	1	34.6	-1.4	9.57	0.1	Na
Vmf4	P	13.06.17	5	Na	Na	63	34.3	1.75	1.15	0.5	657.3
Vmf4	P	13.06.17	25	Na	Na	1	34.5	0.48	1.54	0.6	428.4
Vmf4	P	13.06.17	50	Na	Na	0	34.5	0.1	1.61	0.4	691.2
Vmf4	P	23.08.17	5	Na	Na	20	31.9	5.5	0.00	2.5	100.6
Vmf4	P	23.08.17	25	Na	Na	0	33.5	4.6	0.04	4.8	42.1
Vmf5	P	14.03.17	0	Na	Na	33	34.5	-0.5	10.30	0.1	Na
Vmf5	P	14.03.17	5	Na	Na	16	34.7	-0.7	10.19	0.1	Na
Vmf5	P	14.03.17	25	Na	Na	1	34.7	-0.7	9.90	0.1	Na

1 **Table 2.** Average photosynthetic parameters (with one standard deviation in parentheses) in
2 sea ice algal and phytoplankton assemblages from field observations (FRRf-based parameters
3 only), and from the *in situ* incubation experiment conducted underneath the sea ice (FRRf-
4 and ^{14}C -based parameters). The maximum dark-acclimated PSII quantum yield (F_v/F_m), the
5 absorption cross-section of PSII (σ_{PSII} [$\text{nm}^2 \text{PSII}^{-1}$]), the rate of reopening of PSII reaction
6 centers (τ_{ES} [ms]) and non-photochemical quenching (NPQ_{300}) were derived from FRRf
7 variable fluorescence measurements. Fit parameters ($r\text{ETR}_{\text{max}}$, P_{max} , αETR , α and $E_k\text{ETR}$ and
8 E_k) were derived from either FRRf based FLC curves or ^{14}C -based PE curves. FRRf-derived
9 $r\text{ETR}_{\text{max}}$ [$\text{mol e}^- (\text{mol RCII})^{-1} \text{s}^{-1}$] is the light saturated maximum rate of charge separation in
10 RCII, while the FRRf-derived αETR is the light-dependent increase of charge separation in
11 RCII before saturation [$\text{mol e}^- \text{m}^2 (\text{mol RCII})^{-1} (\text{mol photons})^{-1}$]. ^{14}C derived P_{max} is the light
12 saturated maximum rate of ^{14}C uptake [$\mu\text{g C} (\mu\text{g Chl } a)^{-1} \text{d}^{-1}$]. ^{14}C derived α is the initial light
13 limited slope [$\mu\text{g C} (\mu\text{g Chl } a)^{-1} \text{d}^{-1} (\mu\text{mol photons } \text{m}^{-2} \text{s}^{-1})^{-1}$]. Both FRRf- and ^{14}C -derived E_k
14 is the photoacclimation index [$\mu\text{mol photons } \text{m}^{-2} \text{s}^{-1}$]. Asterisk (*) designates significant
15 differences between sea ice algae and phytoplankton. Na defines “not available”.

	Field observations		<i>In situ</i> incubation experiment			
	FRRf-based		FRRf-based		^{14}C -based	
	Sea ice algae	Phyto-plankton	Sea ice algae	Phyto-plankton	Sea ice algae	Phyto-plankton
F_v/F_m	0.27 (0.12) *	0.34 (0.14)	0.37 (0.06)	0.38 (0.05)	Na	Na
σ_{PSII}	5.1 (1.2)	5.3 (0.9)	5.3 (0.2) *	5.9 (0.1)	Na	Na
τ_{ES}	7.6 (4.8) *	4.7 (1.7)	4.2 (0.4)	3.9 (0.4)	Na	Na
NPQ_{300}	13.0 (7.2) *	4.9 (3.2)	2.4 (0.4) *	1.5 (0.1)	Na	Na
$r\text{ETR}_{\text{max}}, P_{\text{max}}$	31 (23) *	80 (37)	41 (3) *	94 (2)	0.18	Na
$\alpha\text{ETR}, \alpha$	0.16 (0.08) *	0.36 (0.09)	0.34 (0.03)	0.35 (0.07)	0.004	0.009
$E_k\text{ETR}, E_k$	221 (156)	217 (69)	120 (2) *	274 (44)	43	Na

16

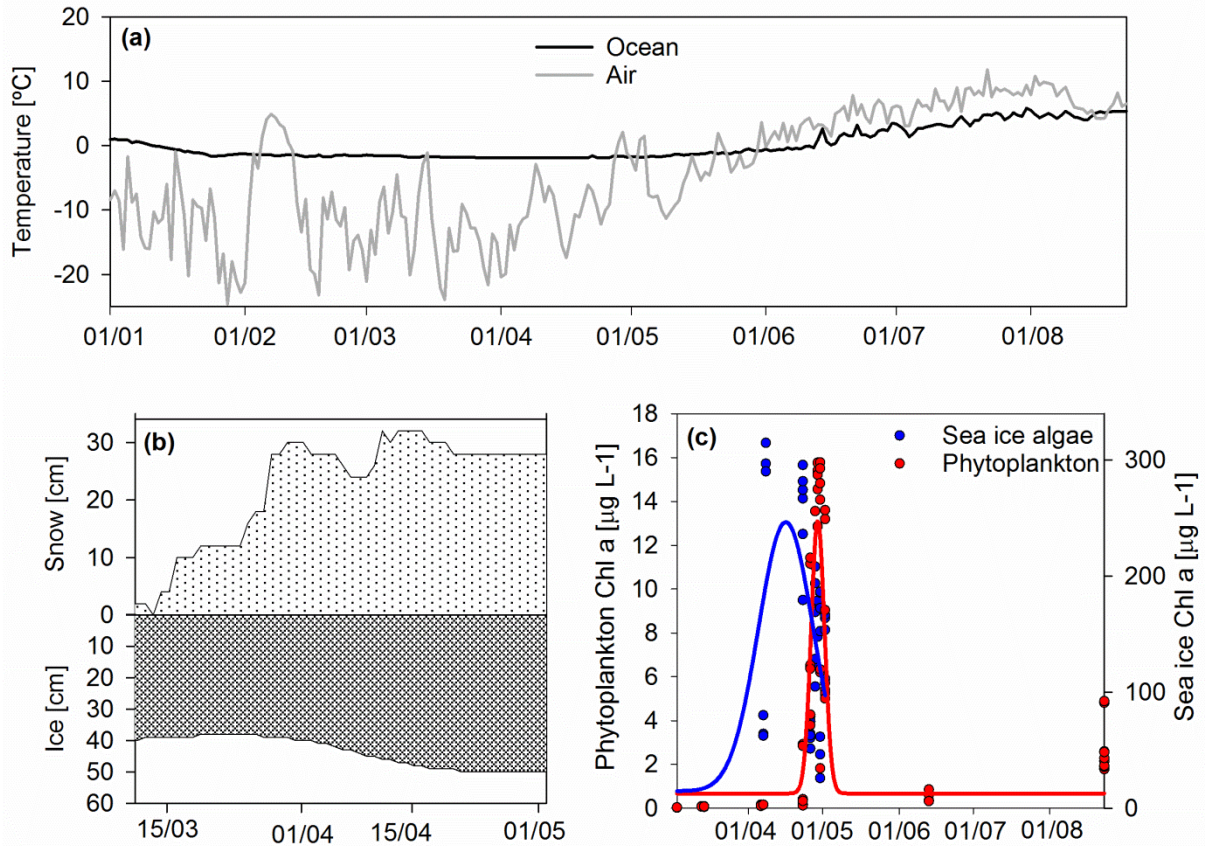
1 **Fig. 1.** Map of Van Mijenfjorden including longitude, latitude and bathymetry (50m
2 resolution). The stations Vmf3 (bottom depth of 80 m), Vmf4 (88 m) and Vmf5 (116 m)
3 are located in the outer basin, which is ~10 km wide and 100 m deep. The inner station (IS; 2 m),
4 intermediate station (IMS; 14 m), main station (MS; 54 m), Vmf1 (78 m) and Vmf2 (61 m)
5 are located in the inner basin, which is 5 km wide and has an average depth of ~30 m.



6

Accepte

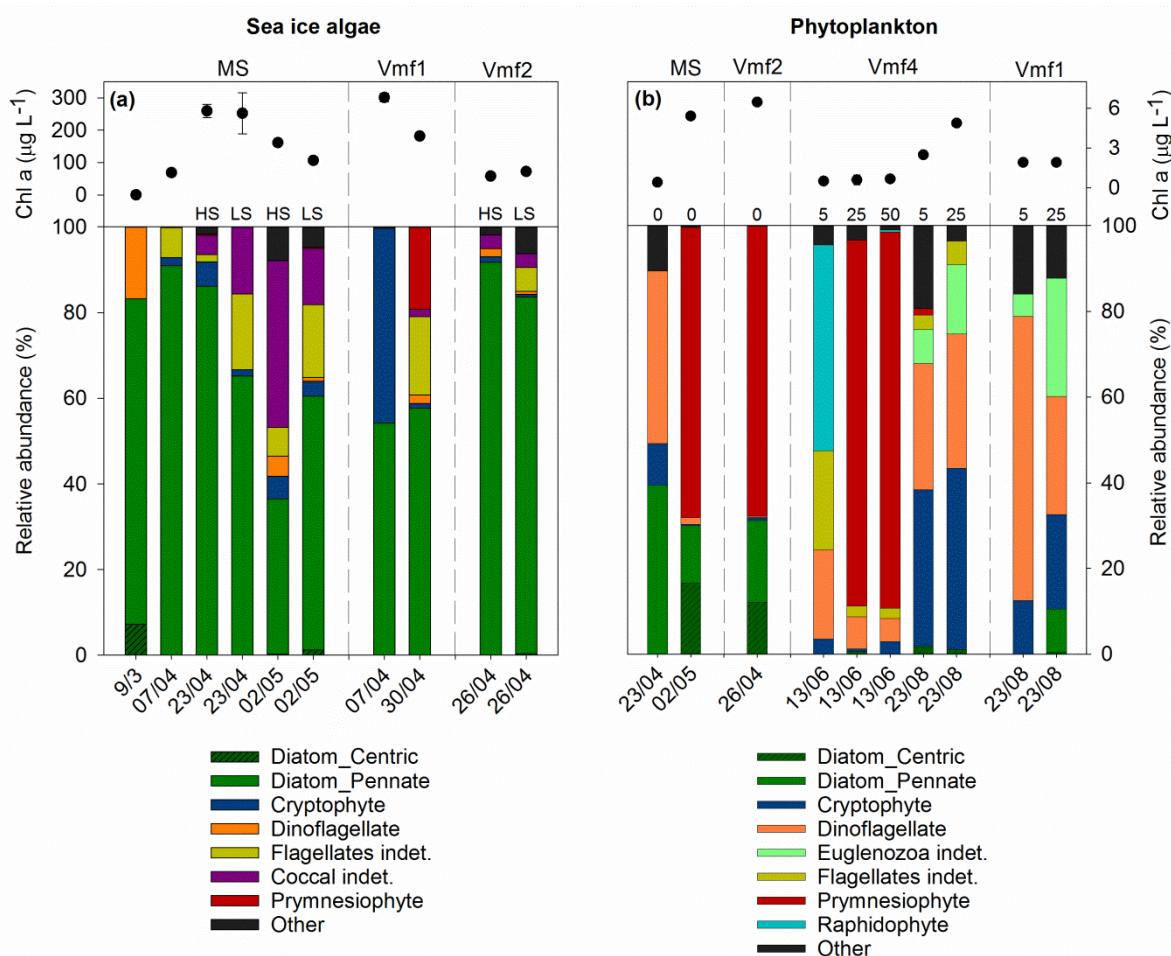
1 **Fig. 2.** Environmental conditions before and during the field campaign in Van Mijenfjorden in
 2 2017; (a) temporal development of ocean temperature (12m depth at Vmf1, retrieved from the
 3 ocean observatory) and air temperature, (b) Temporal development of snow (cm) and ice (cm)
 4 thickness at main station (MS, retrieved from the sea ice observatory) and (c) temporal
 5 development of sea ice algal (blue) and phytoplankton (red) Chl *a* concentrations ($\mu\text{g L}^{-1}$)
 6 during the field campaign. Data points in panel c represent single replicates from different sea
 7 ice cores (sea ice algae) and different depths (0-50 m: phytoplankton).



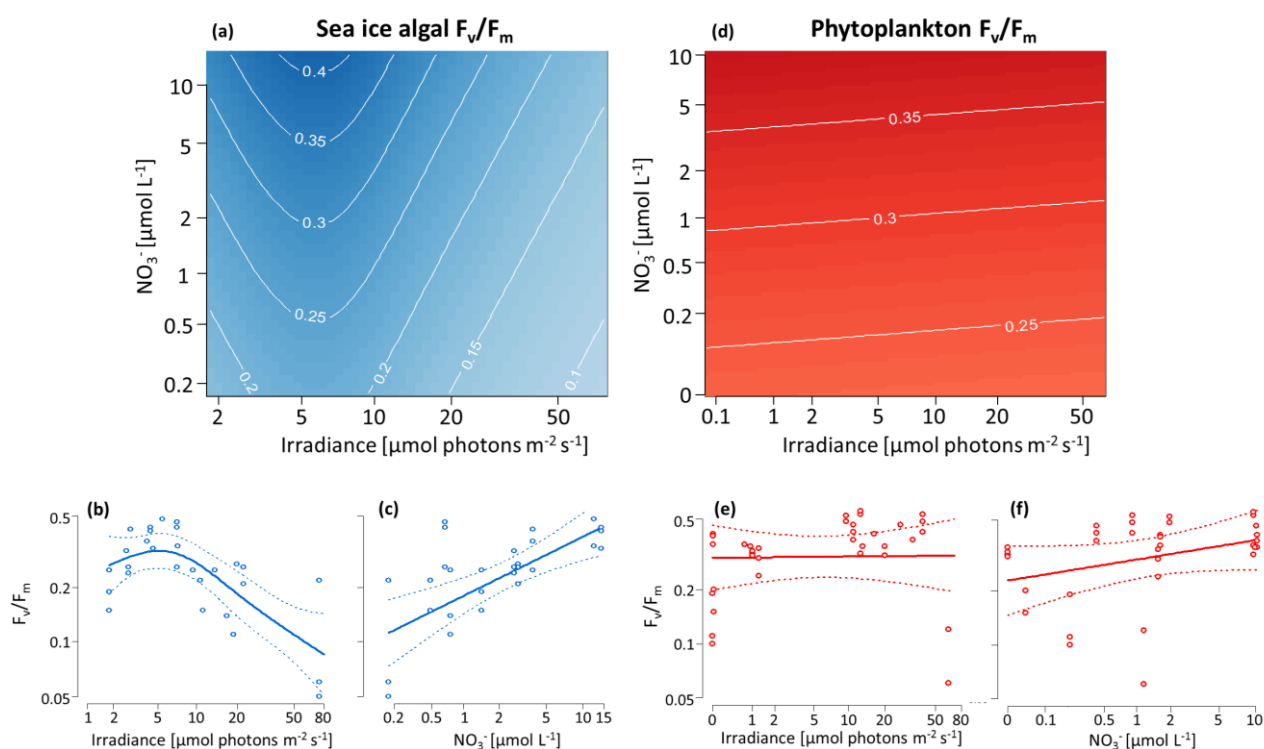
8

ACC

1 **Fig. 3.** Abundance (%) of microalgae groups dominating the sea ice algal assemblages (a;
 2 blue) and phytoplankton assemblages (b; red), as well as Chl *a* concentrations ($\mu\text{g L}^{-1}$) from
 3 the respective cores and depths. The sea ice algal assemblages are divided in stations (MS,
 4 Vmf1 and Vmf2), dates (from 03.03.2017 to 02.05.2017) as well as high (20+ cm) and low (0
 5 - 5cm) snow sites (HS and LS, respectively). The phytoplankton assemblages are divided in
 6 stations (MS, Vmf2, Vmf4 and Vmf1), dates (from 23.04.2017 to 23.08.2017) as well as
 7 water depths (0, 5, 25 and 50 m). Phytoplankton samples from stations MS and Vmf2 were
 8 collected under ice, while samples from Vmf4 and Vmf1 were collected from open water. The
 9 group “Other” includes microalgal groups choanoflagellates, chrysophytes, ciliates,
 10 dictyochophytes, katablepharids, prasinophytes and pyramimonadophytes.



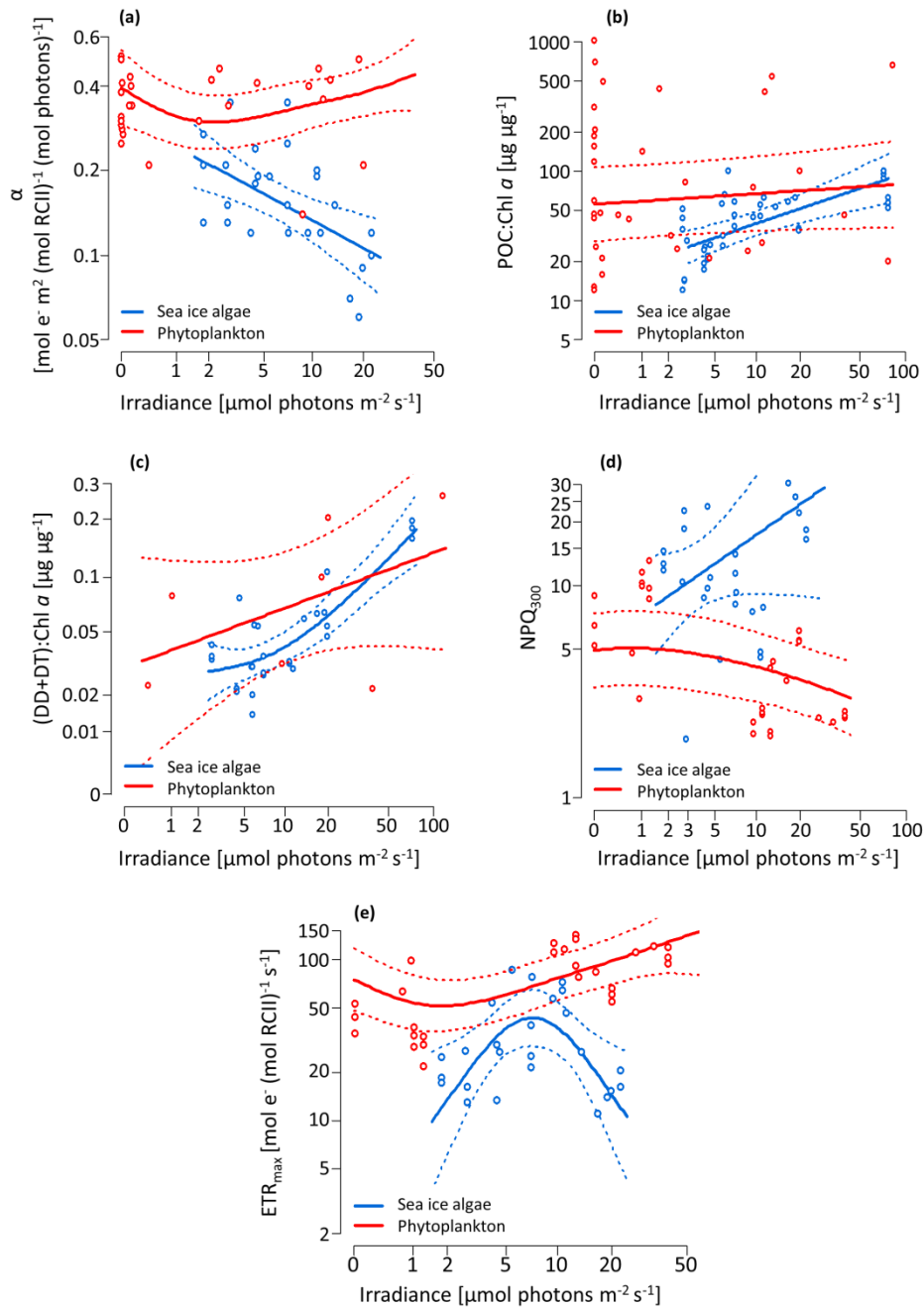
1 **Fig. 4.** Contour plots of the Generalized Additive Mixed Modeling (GAMM) fitted values,
 2 showing modeled changes in the maximum dark-acclimated quantum yield of PSII (F_v/F_m) in
 3 response to daily average irradiance and NO_3^- levels in sea ice algae (a; blue) and
 4 phytoplankton (d; red) algal assemblages. The four bottom graphs show marginal plots for sea
 5 ice algae (b, c; blue) and phytoplankton (e, f; red), where changes in F_v/F_m are separated for
 6 daily average irradiance (b, e) and NO_3^- levels (c, f). Sea ice algae were collected from areas
 7 with varying snow depth (0 – 27cm), and phytoplankton were collected from 0, 5, 25 and 50
 8 meter depths. All variables are log transformed, and in the lower plots raw data values are
 9 shown with GAMM curve fits expressed as solid lines and confidence intervals expressed as
 10 dotted lines.



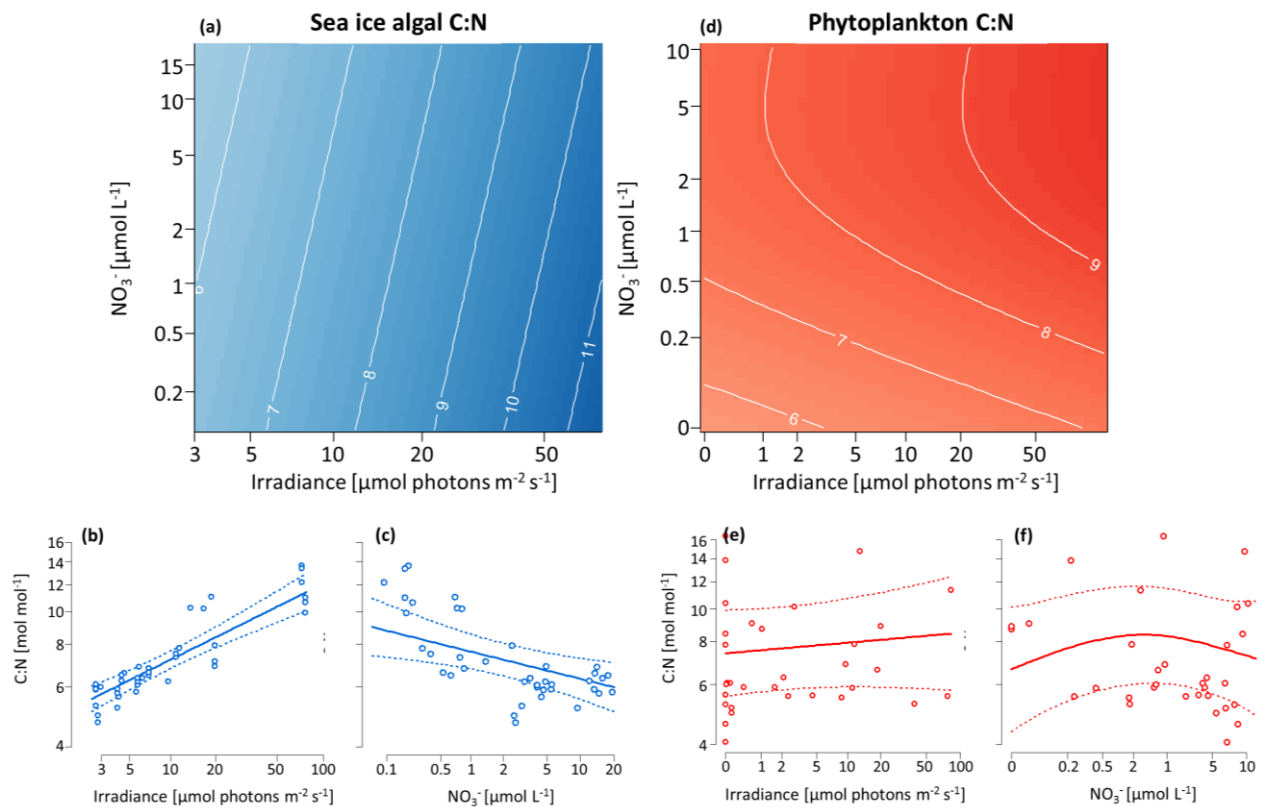
11

12

1 **Fig. 5.** Changes in light utilization coefficient (α ETR; a), particulate organic carbon (POC) to
 2 Chl *a* ratios (POC:Chl *a*; b), maximum photosynthetic rate ($rETR_{max}$; c), light protective
 3 pigment ratios (DD+DT:Chl *a*; d) and non-photochemical quenching at 300 $\mu\text{mol photons m}^{-2}$
 4 s^{-1} (NPQ_{300} ; e) in response to daily average irradiance levels in sea ice algae (blue) and
 5 phytoplankton (red). Sea ice algae were collected from areas with varying snow depth (0 –
 6 27cm), and phytoplankton were collected from 0, 5, 25 and 50 meter depths. All variables are
 7 log transformed, and raw data values are shown with GAMM curve fits expressed as solid
 8 lines and confidence intervals expressed as dotted lines.

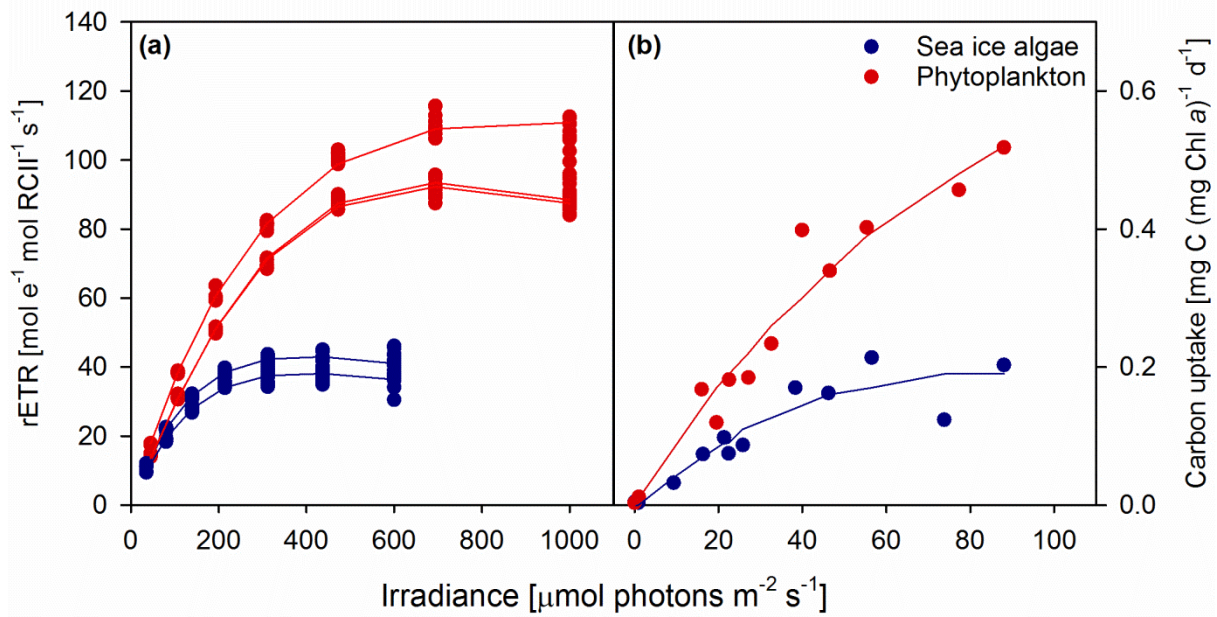


1 **Fig. 6.** Contour plots of the Generalized Additive Mixed Modeling (GAMM) fitted values,
 2 showing modeled changes in the particulate organic carbon to particulate organic nitrogen
 3 ratios (C:N) in response to daily average irradiance and NO_3^- levels in sea ice algae (a; blue)
 4 and phytoplankton (d; red) algal assemblages. The four bottom graphs show marginal plots
 5 for sea ice algae (b, c; blue) and phytoplankton (e, f; red), where changes in C:N is separated
 6 for daily average irradiance (b, e) and NO_3^- levels (c, f). Sea ice algae were collected from
 7 areas with varying snow depth (0 - 27 cm), and phytoplankton were collected from 0, 5, 25
 8 and 50 meter depths. All variables are log transformed, and in the lower plots raw data values
 9 are shown with GAMM curve fits expressed as solid lines and confidence intervals expressed
 10 as dotted lines.



11
 12

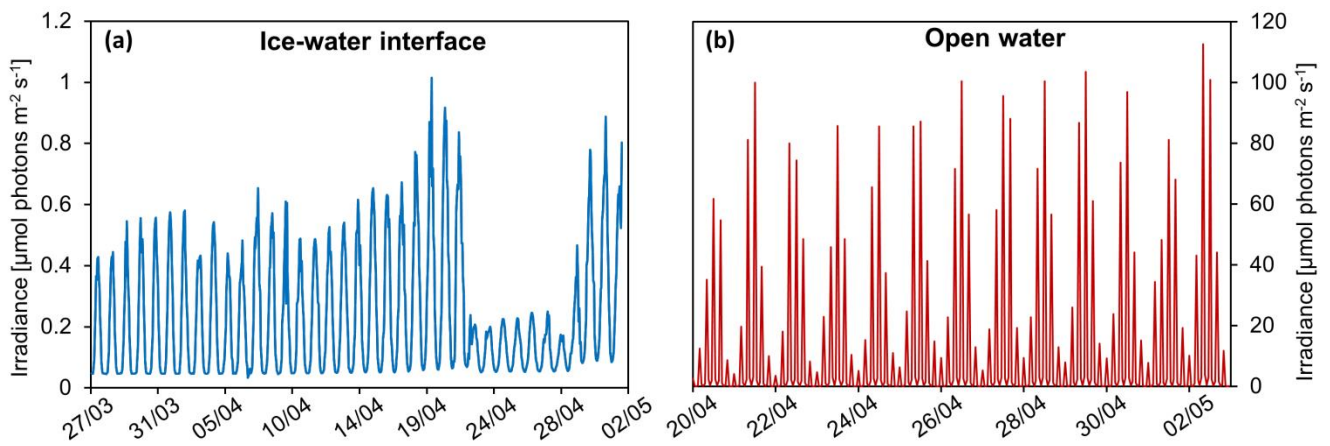
1 **Fig. 7.** FRRf-based FLC curves (a) and ^{14}C -based photosynthesis vs. irradiance (PE) curves
 2 (b) in sea ice algae (blue) and phytoplankton (red) from the *in situ* incubation experiment
 3 conducted underneath the sea ice in Van Mijenfjorden during the main bloom period in both
 4 habitats in 2017. Raw data values of electron transport through photosystem II (rETR; mol e^{-1}
 5 $(\text{mol RCII})^{-1} \text{s}^{-1}$) and ^{14}C -fixation ($\mu\text{g C } (\mu\text{g Chl a})^{-1} \text{d}^{-1}$) are shown as a function of increasing
 6 irradiance and the model fit of Eilers & Peeters (1988) are expressed as lines. Parameters
 7 derived from the FRRf-based FLC curves and ^{14}C -based PE curves are found in Table 2,
 8 while the irradiance regimes encountered by the algal assemblages is found in supplementary
 9 material (Fig. S2).



10

ACCEPTED

1 **Fig. 8.** Temporal changes in the absolute irradiance regimes at the ice-water interface (a; blue)
2 and in open water (b; red). Irradiance at the ice-water interface were retrieved from a Licor
3 LI-192 Underwater Quantum Sensor measuring PAR every hour between 27.03.17 –
4 02.05.2017 at MS. Daily fluctuations of irradiance regimes in open water was modelled and
5 subsequently corrected for PAR measurements retrieved from the ocean observatory,
6 continuously monitoring PAR every second hour at 12 m depth at Vmf1 between 20.04.2017
7 - 02.05.2017. Daily integrated surface PAR (measured in May), a K_d of 0.3 m^{-1} , a mixing rate
8 of 0.003 m s^{-1} and six mixing cycles d^{-1} were used to model daily irradiance regimes down to
9 20 m (estimated from thermocline at Vmf1)



10